

Clinical, industrial, and research perspectives on powder bed fusion additively manufactured metal implants

Lowther, Morgan; Louth, Sophie; Davey, Amy; Hussain, Azad; Ginestra, Paola; Carter, Luke; Eisenstein, Neil; Grover, Liam; Cox, Sophie

License:

Creative Commons: Attribution-NonCommercial-NoDerivs (CC BY-NC-ND)

Document Version

Peer reviewed version

Citation for published version (Harvard):

Lowther, M, Louth, S, Davey, A, Hussain, A, Ginestra, P, Carter, L, Eisenstein, N, Grover, L & Cox, S 2019, 'Clinical, industrial, and research perspectives on powder bed fusion additively manufactured metal implants', *Additive Manufacturing*, vol. 28, pp. 565-584.

[Link to publication on Research at Birmingham portal](#)

Publisher Rights Statement:

Checked for eligibility: 25/06/2019

General rights

Unless a licence is specified above, all rights (including copyright and moral rights) in this document are retained by the authors and/or the copyright holders. The express permission of the copyright holder must be obtained for any use of this material other than for purposes permitted by law.

- Users may freely distribute the URL that is used to identify this publication.
- Users may download and/or print one copy of the publication from the University of Birmingham research portal for the purpose of private study or non-commercial research.
- User may use extracts from the document in line with the concept of 'fair dealing' under the Copyright, Designs and Patents Act 1988 (?)
- Users may not further distribute the material nor use it for the purposes of commercial gain.

Where a licence is displayed above, please note the terms and conditions of the licence govern your use of this document.

When citing, please reference the published version.

Take down policy

While the University of Birmingham exercises care and attention in making items available there are rare occasions when an item has been uploaded in error or has been deemed to be commercially or otherwise sensitive.

If you believe that this is the case for this document, please contact UBIRA@lists.bham.ac.uk providing details and we will remove access to the work immediately and investigate.

Clinical, Industrial, and Research Perspectives on Powder Bed Fusion Additively Manufactured Metal Implants

Morgan Lowther ^a, mxl782@bham.ac.uk

Sophie Louth ^a, sel713@bham.ac.uk

Amy Davey ^b, Amy.Davey@nbt.nhs.uk

Azad Hussain ^c, A.Hussain.3@bham.ac.uk

Paola Ginestra ^{a, d}, paola.ginestra@unibs.it

Luke Carter ^a, L.N.Carter@bham.ac.uk

Neil Eisenstein ^e, eisenstein@doctors.org.uk

Liam Grover ^a, L.M.Grover@bham.ac.uk

Sophie Cox^{a, *}, S.C.Cox@bham.ac.uk

a – School of Chemical Engineering, University of Birmingham, Edgbaston, B15 2TT, United Kingdom

b – Reconstructive Prosthetics North Bristol NHS Trust, Gate 24, Level 1, Brunel Building, Southmead Hospital, Southmead Road, Westbury-on-Trym, Bristol, BS10 5NB, United Kingdom

c – Medical Devices Testing and Evaluation Centre, Institute of Translational Medicine, Heritage Building, Mindelsohn Way, Birmingham, B15 2TH, United Kingdom

d – Department of Mechanical and Industrial Engineering, University of Brescia, Via Branze 38, 25123, Brescia, Italy

e – Royal Centre for Defence Medicine, Birmingham Research Park, Vincent Drive, Edgbaston, Birmingham, B15 2SQ, United Kingdom

* – Corresponding author

Abstract

For over ten years, metallic skeletal endoprotheses have been produced in select cases by additive manufacturing (AM) and increasing awareness is driving demand for wider access to the technology. This review brings together key stakeholder perspectives on the translation of AM research; clinical application, ongoing research in the field of powder bed fusion, and the current regulatory framework. The current clinical use of AM is assessed, both on a mass-manufactured scale and bespoke application for patient specific implants. To illuminate the benefits to clinicians, a case study on the provision of custom cranioplasty is provided based on prosthetist testimony. Current progress in research is discussed, with immediate gains to be made through increased design freedom described at both meso- and macro-scale, as well as long-term goals in alloy development including bioactive materials. In all cases, focus is given to specific clinical challenges such as stress shielding and osseointegration. Outstanding challenges in industrialisation of AM are openly raised, with possible solutions assessed. Finally, overarching context is given with a review of the regulatory framework involved in translating AM implants, with particular emphasis placed on customisation within an orthopaedic remit. A viable future for AM of metal implants is presented, and it is suggested that continuing collaboration between all stakeholders will enable acceleration of the translation process.

1 Introduction

Implantation of metal endoprostheses are increasingly frequent surgical procedures, with hip and knee arthroplasty accounting for over 117,000 surgical procedures in the UK annually. More broadly, skeletal surgeries are the primary procedure for nearly one tenth of all hospital admissions in England ¹⁻³, and around 2 million hip replacements were performed across the Organisation for Economic Co-operation and Development (OECD) in 2015, a 30 % increase since 2000 ⁴. As populations within OECD nations continue to age ⁵ and obesity drives a need for implants in increasingly younger cases, demand for implants is projected to continue rising over the coming decades, with estimates exceeding a 27 % increase in total hip replacements by the 2030s ⁶⁻⁸. Although the complication rate of such procedures is low, there remain significant clinical challenges, which may increase as age and obesity related comorbidities become more prevalent ^{9,10}. Risk of infection initiated at implant surfaces, managing osseointegration, and the inherent mechanical incompatibility of most alloys with bone, represent three of the core clinical issues faced. Alongside the initial debilitation of a patient from these complications, implant revision is typically more costly than the primary procedure and further increases the risk of infection or surgical complications ¹¹⁻¹³.

Currently, the majority of skeletal endoprostheses are produced from titanium (Ti) or cobalt chromium (CoCr) based alloys, which meet the criteria of durability, strength, corrosion resistance and a low immune response ^{14,15}. These characteristics however come at the cost of the high stiffness of these alloys in comparison to bone. Mismatch between the mechanical properties of bone and orthopaedic materials often causes 'stress shielding' in load-bearing implants, where regions of native bone are exposed to reduced compressive or tensile stresses due to the higher stiffness of the implant ¹⁶. This can lead to a reduction in bone density as first formalised by Wolff's law, where bone under reduced stress remodels, in turn causing aseptic loosening of implants resulting in requirement for revision. For load bearing implants, maximising osseointegration to minimise risk of aseptic loosening is a key focus ¹⁷, given that around 20% of orthopaedic revisions within two years are associated with loosening ¹⁸. Osteoblast adhesion is improved by a roughened texture, though the optimum length-scale for this texture remains a matter of some debate ¹⁹. Conversely, for temporary implants or those where removal may be necessary for imaging, such as cranioplasty plates, clinicians may wish to actively minimise osseointegration to reduce trauma to surrounding bone tissue during explantation.

How best to control or influence cell adhesion to an implant is key not only for managing osseointegration. Doing so whilst minimising bacterial adhesion, remains one of the key challenges in modern orthopaedics ²⁰⁻²². Implant associated infections, often referred to as periprosthetic infections (PPI), account for around 22 % of revision surgeries in orthopaedics ¹, and case series have reported infection in up to 30 % of craniomaxillofacial revisions ²³. Such infections are particularly difficult to treat due to formation of bacterial biofilms on implant surfaces ²⁴. Biofilms reduce the efficacy of conventional antibiotic prophylaxis through a range of mechanisms, including the polysaccharide matrix of the film itself, and increased coordination of bacterial populations ²⁵.

Typically, metallic implants have been manufactured by formative techniques such as forging or casting, and subtractive methods for example milling or machining. However, the

past decade has seen increasing interest in using additive manufacturing (AM) techniques, and their potential to enable novel implant geometries or properties to tackle the clinical challenges faced. AM technologies produce parts from 3D data, by joining of raw materials in a layer-by-layer process²⁶. In the field of metal implant manufacture, the most relevant techniques are based upon powder bed fusion (PBF) methods, the basic principles of which are shown in (Figure 1). In PBF, layers of powder are thermally fused by an energy source, such as a laser (L-PBF) or electron beam (EB-PBF). A subsequent layer of powder is spread across the surface and the next cross section of a part fused with the underlying cross section, with this process repeated sequentially until completion. Underlying powder layers provide a degree of support to material above, although supporting structures may be required to stabilise parts during manufacture. Other metal AM methods are available, most notably direct energy deposition (DED) techniques, but the clinical exploration of these methods for biomedical manufacture has been more limited, possibly due to the lower resolution of DED and more widespread commercialisation of PBF. As such, this review focusses on the use of PBF given its current greater clinical relevance.

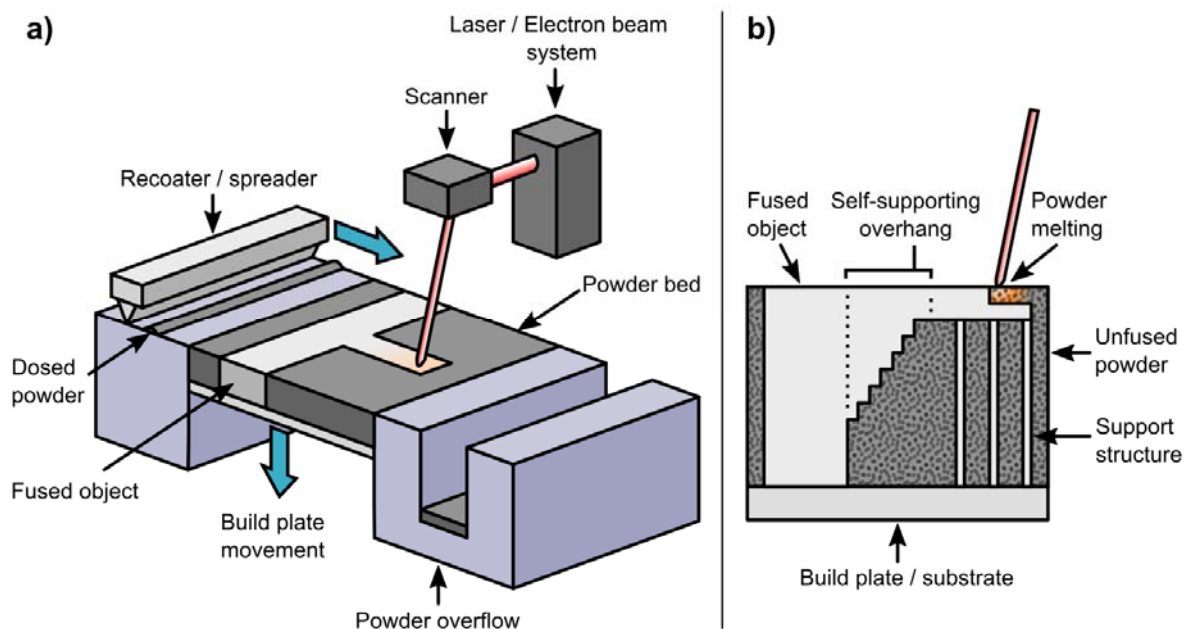


Figure 1 - Schematic showing the principles of powder bed fusion (PBF) additive manufacturing. a) Typical physical layout of PBF apparatus. Dosed powder is spread across a substrate and a cross section is thermally fused by a directed energy source. The build plate subsequently lowers, another layer of powder is spread, and is fused to the material below. b) Cross section of the build region. Unfused powder provides a degree of support to overhanging material, or support structures can be fused as appropriate.

Unlike traditional powder metallurgy processes such as sintering, PBF and DED produce geometrically complex parts with densities exceeding 99.5% without additional post-processing²⁷. In practise, careful process control is required to avoid remnant porosity or defects. With extremely high localised cooling rates, metal AM processes have unique microstructural characteristics. The melt pool in laser PBF, for example, is typically of the order of 200 μm and cools at a rate of over 10^4 K s^{-1} ²⁸. This generates very fine microstructures that are stiffer and have higher yield strength than equivalent cast or wrought materials²⁹.

As a novel manufacturing technique, PBF offers opportunities in enabling new design methodologies and material properties, but also faces challenges in proving it can deliver sufficient clinical benefits to warrant wider adoption. This review seeks to give perspectives on four areas;

1. The current impact of additive manufacturing on clinical practice
2. Opportunities for future clinical advances being made in a research setting
3. Current challenges faced to further industrialisation of AM for endoprostheses
4. Regulatory challenges to widespread adoption of AM implants

Where relevant, advances made outside of biomedical research are discussed in the context of future translation. In doing so, the intention is to provide insight to both research focussed clinicians and researchers in biomedical AM on current clinical practise in metal AM, and the progress being made to translate research.

2 Clinical Impact

In order to better describe the effects of AM on clinical practice, the regulatory division between mass manufactured and patient specific implants can be used to broadly divide the market for endoprostheses. Whilst the dental field has shown rapid uptake of AM, adoption in skeletal fields remains nascent, in part due to the regulatory burdens faced. This assessment of clinical impact therefore focusses on non-dental skeletal applications, as advances in dental AM are summarised by Oliveira et al ³⁰. Though current use of AM for mass manufactured orthopaedic implants is limited, key examples of additional functionality gained and potential economic arguments for adoption are considered. As yet, long-term outcomes for such implants are not available and cannot be discussed in depth.

2.1 Mass Manufactured Implants

The predominant use of AM from a mass manufacturing perspective has been for its osseointegrative properties, with a number of products featuring porous surfaces for long-term fixation (Table 1). The relative dominance of Ti-6Al-4V over Co-Cr-Mo may be because focus has primarily been on non-articulating surfaces, where the higher stiffness of CoCr outweighs its better wear resistance ³¹. This is compounded by the move away from metal-on-metal hip surfaces, where CoCr was particularly favoured. In particular, Ti acetabular cups have been a favoured application of AM, with the first approved designs implanted in 2007, and five-year follow up showing a Kaplan-Meier survival estimate of 99.3 % ³². Spinal interbody fusion implants have also seen widespread adoption across multiple manufacturers, including large companies such as Stryker. Alongside possible osseointegration, roughened surfaces enable friction between the implant and bone for initial stability before bone ingrowth in cementless fixation ³³. Roughened surfaces for fixation can be produced with traditional manufacturing methods, such as use of cast beads on the reverse of acetabular cups and spray coating of fixation surfaces ³⁴. However, the increased design flexibility of AM allows localised tailoring of the mechanical and osseointegration properties within a single process, for example by the use of solid and porous features. The

application of porosity has also been argued as advantageous for decreasing radiographic signature ^{35,36}.

Table 1 - Key examples of commercially mass-manufactured implants produced by AM that have been approved by the FDA ³⁷

Anatomical Region	Product Type	Alloys In Use	Key Features and Clinical Benefits	Manufacturers	FDA Number
Foot & Ankle	Osteotomy truss	Ti-6Al-4V	Porous surface for osseointegration, reduced density for limited radiographic artefacts	4-Web Medical Inc. Additive Orthopaedics	K130185 K170214
Hip	Acetabular cup Femoral stem	Ti-6Al-4V	Porous surface for fixation and osseointegration	Lima Corporation Smith & Nephew Theken Adler Ortho	K141395 K150790 K161184 K171768
Knee	Tibial cavity reinforcement Tibial baseplate	Ti-6Al-4V	Porous surface for fixation and osseointegration	Medacta International Stryker	K170149 K123486
Sacroiliac	Sacroiliac fusion	Ti-6Al-4V	Porous surface for fixation and osseointegration	SI-Bone Inc	K162733
Spinal	Interbody fusion	Ti-6Al-4V Co-Cr-Mo	Porous surface for fixation and osseointegration	Camber Spine Tech. Medicrea Int. S.A 4-Web Medical Inc. K2M EIT Stryker Nexxt Spine LLC NuVasive joimax GmbH HT Medical CoreLink, LLC Renovis	K172446 K163595 K142112 K163364 K172888 K171496 K171140 K172676 K151143 K170318 K162496 K170888

Given that similar porous surfaces can be produced without the use of AM and therefore a lack of any clear step-change in the clinical function, it is key to consider economic justifications for use. From a long-term perspective, AM may improve industrial sustainability both in reducing material wastage, and allowing iterative product redesign without the expense of retooling ³⁸. Though efficiency in material usage by the recycling of powder feedstocks may motivate adoption ³⁹, investment in robust quality control is required to reduce risks associated with reuse. Cost savings may be further offset by the inflated initial cost of powder, given the low yield of many powder production methods within the crucial 15 - 105 μm size range ^{40,41}. Further, arguments regarding iterative product redesign may be less valid in the context of orthopaedic implant manufacture, as in practise any redesign of an implant could necessitate resubmission to regulatory bodies. The highly specific nature of orthopaedic implant regulation counters the conventional wisdom that AM will be disruptive in providing customisation on-demand for mass-manufactured products ⁴². To do so would require a significant shift in the distinction between standardised and patient specific implants, which as discussed in Section 5 is a key cornerstone of existing regulatory frameworks.

Alternative arguments for adoption consider effects in disrupting conventional manufacturing supply chains, reducing lead time. The significance of this for mass manufactured implants

remains to be established, particularly when taking into account that the post processing of AM products can be more complex than for conventional manufacturing. Specific to implant manufacture, the promise of distributed manufacture may allow new cost models for implant supply, particularly where hospitals partner directly with manufacturers⁴³, though the regulation of multiple manufacturing sites and their supply chains may prove a barrier to this.

In summary, whilst AM has seen adoption for mass manufacture of implants and mid-term outcomes are currently positive³², data for long-term outcomes are needed to demonstrate additional clinical benefit. Current adoption is likely being driven by a range of economic factors, and consideration of possible future benefits and the risk of falling behind the adoption curve of new technologies. The adoption of AM in dental implant manufacture may represent a model of industrial uptake, with initial pioneering work performed in the late 1990s followed by a broader recognition of the advantages in the flexibility of manufacture and wider uptake^{44,45}.

2.2 Patient Specific Implants

Commonly referred to as 'custom' implants, patient-matched or patient specific implants (PSIs) are defined as those designed and produced for use in a specific individual. From a regulatory perspective, there are two key approaches to such implants: those that fit a broad 'envelope' of design features whilst allowing greater flexibility in the size or shape of specific design elements than mass manufactured implants, and those that are uniquely 'custom' and produced for atypical clinical needs where it would be infeasible for a design envelope to exist^{46,47}.

Examples of envelope type implants include cranioplasty plates and typical craniomaxillofacial (CMF) applications, where a sufficiently large market has been developed to sustain small scale manufacture, but where fixed size or modular implants are inappropriate. Cranioplasty plate manufacture is presented as case a study in Section 2.3 to demonstrate how AM has altered the workflow of implant design and manufacture in a clinical setting. From an economic perspective, estimation of the market share for additive manufactured PSIs is difficult, with much more limited data collection for cranioplasties in comparison to orthopaedic joint registries^{48,49}. Currently across Europe, several hospitals and implant manufacturers have reported their use of AM for custom prostheses, but exact details of the extent of this uptake remain unknown^{50–52}. Positive uptake has also been observed within the dental industry, particularly for the manufacture of CoCr dental crowns and bridges⁴⁵.

For uniquely customised implants beyond specific CMF reconstructions, AM implants have seen particular use in treatment of bone tumours, such as giant cell tumours or sarcomas, which severely affect anatomy for which no existing modular implants are available. Patient specific clavicle, scapula, and pelvic implants have all been demonstrated (Figure 2) and resulted in patients showing optimal Musculoskeletal Tumor Society 93 (MSTS93) scores over a three year follow-up period⁵³. Positive results have also been achieved for anatomical regions where existing implants limit joint function or where large volumes of bone have been resected, affecting stability, such as irregularly shaped massive tibial

defects⁵⁴. A series of four proximal tibia blocks demonstrated the advantages of AM over conventional techniques, allowing use in conjunction with a standard knee prosthesis whilst including a porous surface structure where ligaments can be directly sutured³⁸.

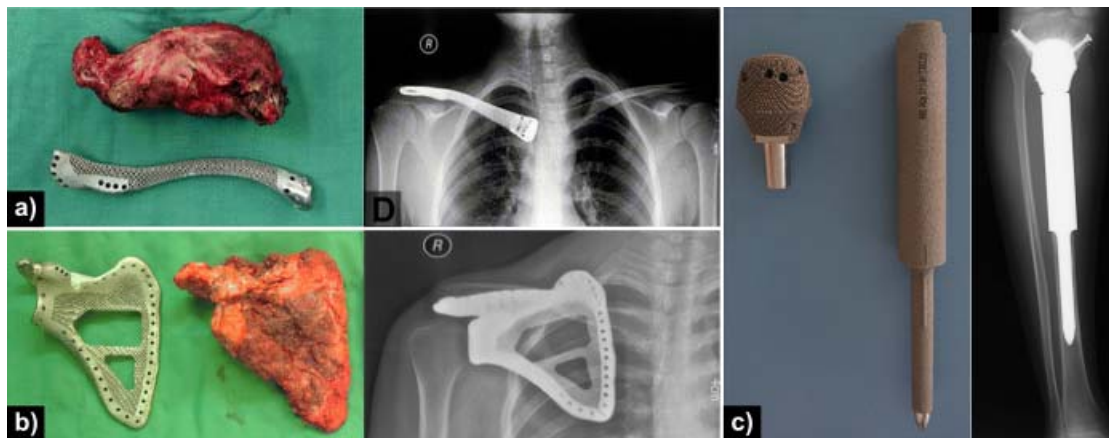


Figure 2 – Examples of AM patient specific implants used for reconstruction of resected bone tumours and follow-up x-ray films showing placement, specifically a) clavicle, b) scapula, and c) uncemented proximal tibial reconstruction^{52,53}.

Across all anatomical sites, the overarching process of designing AM implants is heavily digitised, transferring patient scan data from MRI or CT to design software, allowing direct replication of patient anatomy. One current approach is based on the mirroring of healthy anatomy to replace a defect, restoring symmetry that has been lost through trauma or resection^{52,54}. This process also has advantages in surgical planning, with the ability to produce low-cost 3D printed polymer models of the implantation site from the same scan data, which can in turn be used to plan surgical management⁵⁵.

2.3 Case Study: AM Cranioplasty

Conventional patient-specific cranioplasty plates are cut from titanium sheet and pressed onto a model of the defect region. This pre-forming model is typically manufactured manually using patient CT data. A physical model of the defect region is produced by 3D printing in a polymer, and the defect manually recontoured by moulding of clays. From this, a dental stone pre-form is made onto which the titanium sheet can be pressed and moulded. Use of custom plates manufactured in this way has shown favourable outcomes in comparison to allografts, autografts, or alternative alloplasty materials including those shaped during surgery such as titanium mesh or polymethylmethacrylate^{23,56}.

Typically, a period of at least 3 months is kept between craniectomy and cranioplasty, though this waiting period may be up to 2 years where patients are not yet neurologically stable^{23,57}. However, duration of pre-operative complications between the onset of a cranial defect and the cranial plate insertion is a significant complaint amongst patients⁵⁸, and there remains conflicting evidence of whether shortening the period between craniotomy and plate cranioplasty negatively affects patient outcome; systematic review of literature by Tasiou et al found that later cranioplasty may minimise surgical complications, but early cranioplasty indicated improvement in key post-operative indicators and reduced overall hospital stay

duration^{59–63}. Though rapid manufacturing using AM could in principle reduce this waiting period, given the current practice in delaying cranioplasty, this has not yet been the case. Rather than shortening the total waiting period, AM has had a high impact minimising time at the later clinical stage post-craniotomy, once a patient's condition is sufficiently stable to consider cranioplasty. As traditional cranioplasty manufacturing takes up to 4 weeks, plates are typically ordered, manufactured, and sterilised prior to scheduling of surgery. At any point between the commissioning of a cranial plate and completion of manufacture, a patient's clinical need may change such that the originally manufactured plate is no longer appropriate. This wastes both material and prosthetist time, as shown in the 'conventional' branch of the process diagram (Figure 3).

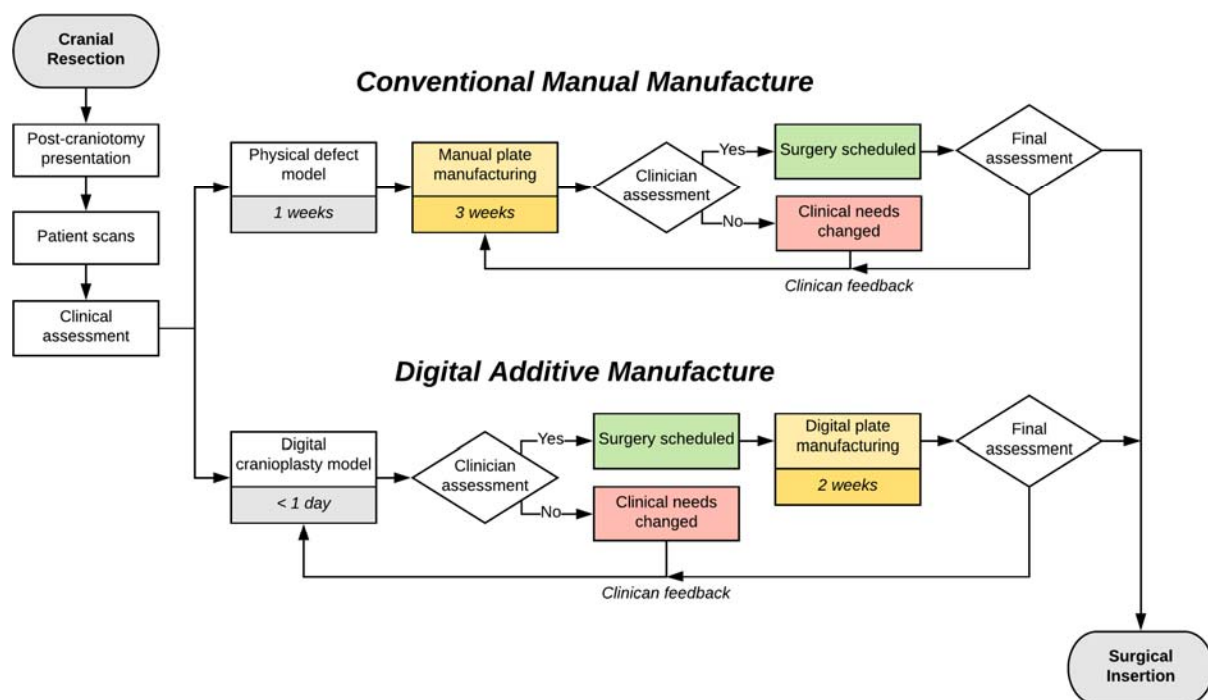


Figure 3 - Schematic of the processes-flow to manufacture a custom Ti cranioplasty by conventional, manual means versus by a digital, additive manufacturing process.

In comparison, AM allows manufacture of cranial plates at a later stage in the process chain. A digital model of the cranial plate can be produced within hours by an experienced prosthetist, which can then be viewed by surgeons and other clinicians the same day. This design is archived and once a surgical date is confirmed, manufacturing can start, and a plate delivered for sterilisation within 2 weeks⁶⁴. By shifting to manufacture post-surgical scheduling, the likelihood of a plate no longer being required is reduced, cutting waste. This alteration of supply chains and introduction of lean manufacturing is similar to the supply chain effects observed in more general manufacturing settings^{65,66}. Crucially, plates manufactured using both fully and semi-automated digital workflows show superior accuracy to conventional hand-manufactured plates, reducing the need for adaption during surgery⁶⁷. Greater surgical duration has been associated with poorer patient outcome⁶⁸, and whilst it is difficult to unpick the association between operative time, complications during surgery, and post-operative complications, the importance of minimising surgical time and related anaesthesia duration has been highlighted in several surgical fields^{69,70}.

Despite the potential benefits in both precision and efficiency, there are however barriers to the widespread use and adoption of this digital approach at national, regional, and hospital level. Across multiple UK industries, provision of appropriate investment and training in the application and use of AM has been identified as a common hurdle ⁷¹, whilst studies of national healthcare providers across Europe have shown uptake of novel technologies is highly dependent on hospital funding at a regional level ^{72,73}. In a clinical setting, surgeons and consultants unfamiliar with these new methods will be cautious to adopt them until there is strong evidence for improved patient outcome ⁷⁴. This may particularly be driven by required changes in surgical technique. For example, plates produced by L-PBF require more precise positioning due to a higher yield strength than conventional plates, which can be manually deformed during surgery to fit. This reduced formability is in part due to the finer grained metallurgical structure and the higher thickness of L-PBF plates, reported as up to 3 mm ⁷⁵ versus the sub-mm thickness of traditional pressed prosthetics ⁵⁶. To overcome this reduced adaptability of the plate during surgery, custom cutting or mounting guides can be provided ⁷⁶, and whilst this involves adjustments to surgical technique, in complex cases can reduce surgical duration ^{49,77}.

3 Future Clinical Benefit

Currently, there is a large volume of research being generated at every stage of the AM implant chain - from the materials produced by the process, to the design of implants and the additional processes after AM needed to produce a device suitable for implantation. Whilst there are many steps before these innovations can be translated to clinic, progress is being made against several of the core clinical challenges faced. Immediate benefits can be obtained through the greater flexibility of design enabled by AM. Opportunities are presented for new design strategies at a mesoscale and macroscale, with focus given to their use for osseointegration and reduced stress shielding respectively. Implants with secondary clinical functions that could be manufactured by PBF processes are also discussed. Further to this, the long-term development of materials possible through AM is considered. With the ability to rapidly prototype different implant alloys by altering feedstock, geometrically complex samples of novel alloys can be produced without the need for specialist casting facilities, and in small quantities. Efforts to produce alloys with low modulus and high strength are considered, alongside the production of bioactive or resorbable alloys.

3.1 Design Optimisation

AM allows manufacture of geometries previously considered unfeasible, the most apparent example being reliable creation of designed lattice structures. Taking advantage of this capability allows entirely new implant features and functions to be created, meeting a range of clinical challenges head-on. Particularly for load-bearing implants, ensuring stability for long-term fixation is a key clinical target. At a mesoscale (at the interface between sub-millimetre microscopic scale, and the macroscopic scale where an objects mechanical properties can be reliably modelled with continuum mechanics), tailoring porous structures to encourage osseointegration is discussed, including an overview of the relevant studies using AM materials. Moving beyond to macroscale design of implants, strategies for minimising

stress shielding using lattices are assessed. Using the flexibility of AM to enable novel implant functions is also discussed, with an emphasis on incorporation of a second functional component or material.

3.1.1 Mesoscale Design for Osseointegration

The high resolution of powder bed processes enables design of implant behaviour at the mesoscopic manufacturing scale – considered as between microscopic sub-millimetre and macroscopic scales – with production of lattice structures a clear example. Porous structures are difficult to produce through conventional implant manufacturing techniques, having required production by powder metallurgy routes ⁷⁸, and with little regularity or control of the resulting pore structure. Additive manufacturing allows for creation of controlled or ‘engineered’ porosity, potentially enabling direct osseointegration ¹⁷ whilst simultaneously reducing the effective bulk stiffness of material or implants ⁷⁹. Enhancing osseointegration is a key area of study to ensure implant stability, particularly given the increase usage of cementless hips versus cemented since 2003 in the UK ¹. Despite continuing improvements in design, cementless implantation continues to be associated with a higher revision rate from 1-10 years compared with cemented and it has been hypothesised that enhanced osseointegration may improve medium to long-term outcomes ^{1,18}.

Relevant pore characteristics and their effect on osseointegration have been studied extensively in AM materials, highlights of which can be found in Table 2. An optimum minimum pore size is frequently cited as 100 µm based on early studies of the phenomenon in ceramics ⁸⁰, with a maximum pore width below 1000 µm ⁸¹, and subsequent studies in porous metal substrates have focussed on this regime. Studies that have maintained a fixed pore size, indicate that greater ingrowth occurs at higher total porosity ⁸², whilst pore shape has not been found to influence osseointegration directly but may direct cell growth and differentiation *in vitro* ^{83,84}.

Table 2 – Collated data on the influence of pore size on osseointegration in additively manufactured materials.

Alloy	Pore Size Range (µm)	Tissue	Duration	Outcome	Source
Ti-6Al-4V	160 - 660 200 - 700 500 - 1000 450 - 1200	Goat - spinal cages Human osteoblasts Human periosteum cells Human osteoblasts	12 weeks 2 weeks 2 weeks 6 weeks	Greatest bone ingrowth observed around 200 µm pore size. Smaller pores show reduced reconstruction and lower proportion of lamellar bone.	⁸² ⁸⁵ ⁸⁴ ⁸⁶
Commercially Pure Ti (cp-Ti)	100 - 800 300 - 900	Human osteoblasts Rabbit femoral condyle and tibia metaphysis	12 weeks 8 weeks	Greatest fixation ability observed at 600 µm <i>in vivo</i> . At pore sizes below 200 µm, osteoblasts bridge pores.	⁸⁷ ⁸⁸
Tantalum	200 - 2000	Human osteoblasts	11 days	Greater ingrowth seen with decreasing pore size towards 200 µm.	⁸⁹

Whilst an ideal pore structure has yet to be evidenced, *in vivo* research has demonstrated improved osseointegration of porous metallic implants compared to conventional materials. Multiple studies of porous Ti lumbar fusion cages in an ovine model have demonstrated significantly higher osseointegration than both conventional polymer, and titanium coated polymer alternatives^{90,91}. Several manufacturers now utilise AM in the production of spinal fusion implants, as identified in Table 1, both in Ti and CoCr based alloys. Whilst the greater osteoconductive properties of Ti alloys over CoCr are well established⁹², both materials have shown long-term osseointegration in lattice structures. Similar patterns of bone formation have been demonstrated for both Ti-6Al-4V and CoCr in an ovine femoral model, with higher surface contact between bone and Ti shown but a greater osteocyte density at the periphery of the CoCr network indicating a slower remodelling process⁹³. The opportunity to improve osseointegration and reduce the stiffness of CoCr alloys is particularly important, given the higher stiffness and resulting tendency for stress-shielding.

To support the development of these engineered porous structures, osseointegration and relevant characteristics must be modelled in large defects, including for lattices with deliberate variation in pore properties. Considering behaviour across pore structures may prove key to maximising integration. Flow behaviour when seeding onto AM gradient pore structures has been shown to be crucial, with gradually reducing cell density and actin expression as pore size decreases deeper into a gradient lattice⁹⁴. Experimentally validated modelling tools have indicated that both the pore size and surface roughness at a micron scale control flow, and may be used to tailor it⁹⁵.

3.1.2 Macroscale Implant Design for Stress Shielding

For a given set of design constraints, such as volume and mechanical function (referred to as a 'design space'), AM enables far greater freedom than conventional manufacturing techniques. In particular, this allows for optimisation of the stress distribution within an implant and its effect on the defect site, reducing stress shielding and interfacial motion at the bone interface, minimising the risk of aseptic loosening⁹⁶.

Topological optimisation has been widely explored as an approach to redesigning parts for AM to make use of this design freedom, within a given design space. Typically such techniques are free to attain any shape within loading constraints, however within a biomedical context it is key to consider the anatomical site, and resulting overall shape of an implant as a constraint⁹⁷. Optimisation methods often rely upon a theoretical variation of material behaviour within this envelope for modelling purposes, for example reducing the local density of material where appropriate to reduce stiffness⁹⁸, or varying material composition⁹⁹. Gradients of composition within PBF techniques are not possible¹⁰⁰, so in practice this variation of material behaviour across an implant - commonly referred to as a functionally graded material¹⁰¹ - can be most easily achieved by the use of varying porosity and lattice structures¹⁰². The principles of applying topological optimisation and functional grading to implants using lattices, and the AM specific manufacturing challenges involved, are discussed in depth by Wang *et al*¹⁰³. Suffice to say, it is key to include specific manufacturing constraints such as minimum feature size and the angle at which material can 'self-support' within any topological optimisation algorithm.

Reduced stress shielding achieved through functionally graded lattices has been modelled in several key clinical contexts, including hip arthroplasty femoral stems^{104,105}, and knee arthroplasty tibial components¹⁰⁶. Given that the loading of such implants lies primarily along the stem axis, *in vitro* models have focussed on radial grading of lattices¹⁰⁷. Stem models featuring both closed outer surfaces¹⁰⁸, and open radial grading with high porosity at the extremities to transfer stress to surrounding tissue¹⁰⁹, have been manufactured and mechanically assessed to show improved stress distributions in comparison to solid stems. However, relatively few full-implant models have been manufactured to demonstrate improved stress distribution in practise. Initial *in vitro* testing in a femur model has shown promise, potentially reducing secondary bone loss through stress shielding by 75% compared to an equivalent solid implant¹⁰⁵.

Physical modelling and iteration remains necessary to optimise response even for comparatively simple structures, as use of a porous core without lattice grading shows significant reduction in flexural stiffness beyond that predicted by computational modelling¹¹⁰. The mechanical behaviour of complex graded lattice structures is not easily modelled outside the elastic deformation regime, making it difficult to accurately predict failure behaviour beyond bulk or global deformations. In order to better understand lattice failure, simple linearly graded structures have been widely studied *in vitro*^{111,112}. Under compression, sequential collapse of layers prior to full densification of structures has been observed in graded lattices, both with linear and curved gradients in density, with no significant difference in the mechanical response to static and dynamic compression testing^{113,114}. The degree of densification between layer failures can be modified, as demonstrated by structures using sigmoidal density gradients¹¹⁵. This may reduce the risk of a catastrophic collapse of multiple layers of a lattice.

Lattice designs face challenges when applied to implant geometries, particularly at the edge of the implant where unit cells will not naturally terminate. Simplistic trimming of unit cells at edges with no change in geometry potentially leaves unprintable or mechanically unstable structures. Four key approaches to this challenge are represented in Figure 4, each of which has clinically relevant impacts on behaviour of a structure. The addition of an outer 'skin' to support edge cells has been proposed, with the additional stiffness producing a form of functional grading (Figure 4b)¹⁰⁷. In certain clinical contexts, the resulting retardation of osseointegration may be considered positive, particularly if revision of the implant is considered likely¹⁰⁶. Where it is desirable to maintain an open lattice for osseointegration, net-based skins may provide mechanical support without significantly reducing access to the lattice for post processing¹¹⁶, though these designs are computationally more complex to produce (Figure 4c). Alternatively, several computational methods have been proposed to counter edge effects by deforming lattice cells to conform to the desired geometry. In the 'swept' method, the whole unit cell structure is deformed, however this only works for simple edges and can significantly alter mechanical behaviour (Figure 4d). Use of a meshed method alters unit cells in shape and size with finite element analysis to preserve mechanical properties, but again sacrifices the original unit cell geometry (Figure 4e)¹¹⁷.

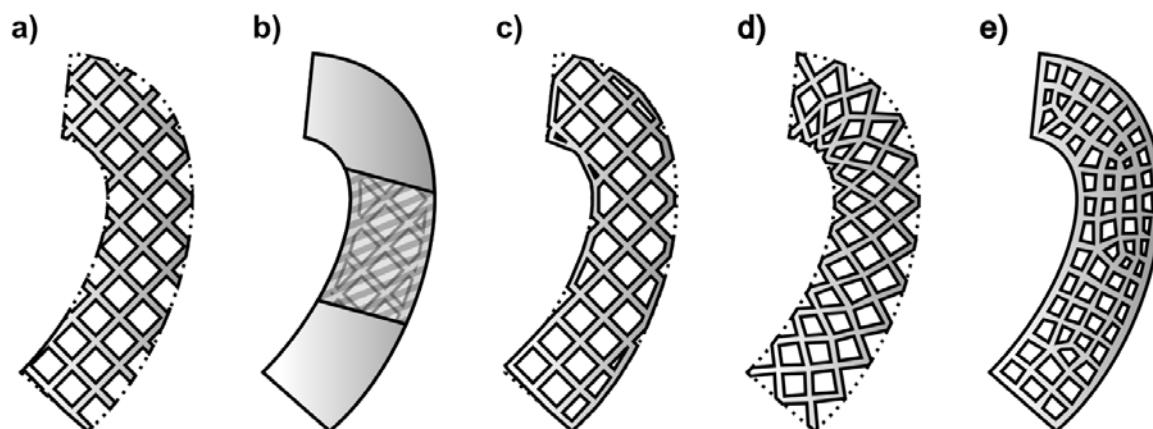


Figure 4 - Methods for adapting a) a simple lattice structure, to prevent hanging edges. From left to right: b) solid skin encasing the entire lattice, c) net skin joining key lattice segments, d) swept method of deforming lattice cells, and e) meshed method of deforming cells. Adapted from ¹¹⁷.

3.1.3 Functional Implants

Beyond the properties of a metal implant itself, AM can be used as an enabler for other technologies, such as localised delivery of therapeutic agents. Given that infection and aseptic loosening account for over 40 % of hip revision surgeries recorded over a 16 year period ¹⁸, the ability of an implant to elute antimicrobials or osseointegration-related factors is worth exploring. Coatings are well established as effective for both antimicrobial ¹¹⁸, osseointegrative properties ^{119,120}, but may be limited in duration of therapeutic efficacy and durability both prior and post implantation.

One example of an alternate AM-enabled approach to the delivery of therapeutic agents is to consider the delivery vehicle as a distinct second phase integral to the implant (Figure 5). Intercalation of an eluting phase within a lattice structure may be a way to combine stress matching, therapeutic effects, and improved osseointegration in one implant ¹²¹. This basic proof of concept has been established in cp-Ti with a range of biocompatible fillers ¹²². Infiltration of a simvastatin loaded hydrogel into a Ti-6Al-4V scaffold showed significantly greater vascularisation, osseointegration, and bone ingrowth in a rabbit model compared to equivalent structures without a secondary phase ¹²³. Alternatively, a larger and more controlled volume of material may be delivered by integrating the second phase inside a physical reservoir, i.e. a hollow implant. In this way, the release characteristics of the therapeutic agents can be tailored both by altering the characteristics of the delivery vehicle, and by modification of the implant pore structures through which elution is achieved ^{124,125}. Addition of permeable membranes on the outside of a porous implant could further optimise elution, and enable loading of the eluting agent prior to implant insertion ¹²⁶.

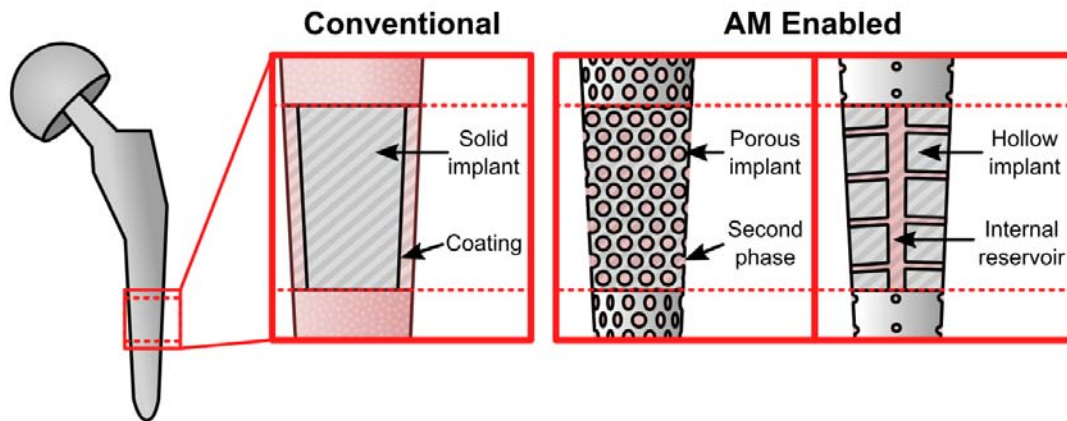


Figure 5 - Schematic visualising three approaches to adding therapeutic materials to an implant to achieve additional functionality; conventional addition of a coating, intercalation with an AM lattice structure, and inclusion of an internal reservoir through AM.

The ability to more easily generate hollow or porous structures may also enable the deployment of integrated sensors. Advances in implantable sensors have as yet been driven primarily by glucose monitors or cardiovascular implants^{127,128}. Whilst there are challenges in preventing fouling of sensors and retaining analytical accuracy¹²⁹, a range of advances have been made that make long-term implantable sensors more viable as discussed by Vaddiraju et al¹³⁰. Where implanted orthopaedic sensors have been demonstrated, mechanical load data has been measured, which does not require contact between the sensor and native tissue, preventing biofouling by encapsulation of the device within the femoral neck. Potentially serious deficiencies in existing mechanical testing regimes for hips were established by measurement of contact forces and moments within a hip implant, measuring *in vivo* forces with greater magnitude and varying orientation compared to ISO standards¹³¹. Moving towards in-situ measurement of key post-operative markers for inflammation may provide greater resolution than blood measurements, further building on improvements in identifying peri-prosthetic infection¹³².

3.2 Alloy Development

Implanted biomedical alloy choice is restricted, with a narrow range of Co-Cr alloys and Ti alloys dominating. Novel alloys have been explored by a range of manufacturing methods¹³³, but development is typically time consuming and requires specialised equipment, with difficulties in creating complex geometries limiting the use of materials such as NiTi¹³⁴. Due to the powder feedstock that PBF processes are reliant upon, it is possible to create and validate entirely new alloys either by pre-alloying during atomisation of powders, or simply by blending of feedstocks. A range of compositions can be rapidly assessed at lower expense, by mixing elemental or alloyed powders such that localised homogenisation of the alloy occurs during the AM process¹³⁵. Two broad subsets of alloy are considered; those with low modulus to minimise stress shielding, and 'bioactive' alloys that emit therapeutic materials or are resorbed with time. Validating a broader range of materials will increase design flexibility, and enable selection of materials to be better informed by clinical need and not only availability. Note however, that development of new materials should be considered a long-

term goal given the complexity of validating alloys as safe for biomedical use, particularly when implanted for extended periods of time.

3.2.1 Low Modulus Alloys

One approach to reducing the stress-shielding problem has been the development and testing of novel, low-stiffness alloys¹³³. Finite element modelling of these materials versus conventional alloys has shown significantly lower 'stress-jump' at the implant-bone interface¹³⁶, which in turn will reduce stress-shielding and is one motivator for their use. Particular focus has been dedicated to metastable beta phase titanium alloys due to the high biocompatibility of Ti. A new series of such alloys have been produced by AM, and the elastic modulus and tensile yield strength of these materials is shown compared to Ti-6Al-4V and cp-Ti (Figure 6). Note that though yield strength is reduced in comparison to Ti-6Al-4V, significantly lower elastic moduli are achieved whilst retaining strength above that of cp-Ti. In most cases, these alloys have used a modification of previously developed TZNT (Ti-Zr-Nb-Ta) and TMZF (Ti-Mo-Zr-Fe) systems, whose biocompatibility is well established. These developments have not been limited to solid components; multiple authors have reported the fabrication of implantable scaffolds from low modulus alloys^{137–140}. The use of lattice or scaffold structures, enables further optimisation of mechanical response including reducing the effective stiffness of an implant, as discussed in Section 3.1.2. Whilst these results are significant for approaching the modulus of healthy bone, it is worth noting that the low effective modulus can be induced by unintentional or process induced porosity^{79,141}, which could prove problematic for fatigue strength.

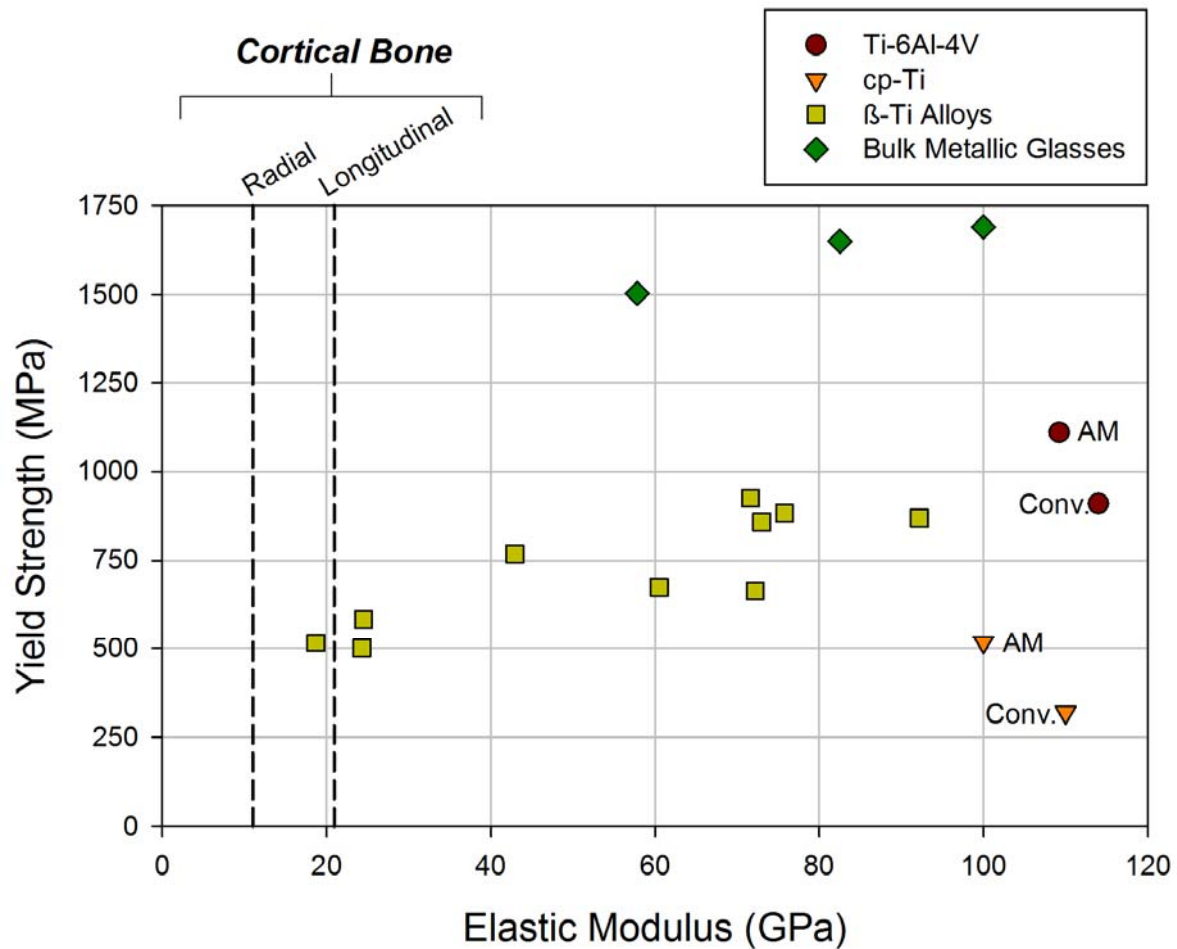


Figure 6 - Graph showing the tensile properties of additively manufactured low-modulus alloys in comparison to conventionally and additively manufactured Ti-6Al-4V and cp-Ti, and the elastic moduli of cortical bone. Reduction in stiffness correlates with a reduced yield strength for beta phase titanium alloys compared to Ti-6Al-4V, whilst metallic glasses show enhanced strength^{141–152}.

The tribological behaviour of these newly developed alloys has yet to be investigated, which may prove a significant barrier to use. For example, though the TMZF system was commercialised for modular femoral stems by Stryker, they were recalled in the United States by the Food & Drug Administration (FDA) in 2011 due to excessive wear degradation¹⁵³. The anomalous behaviour has been linked to the low strain hardening behaviour of the alloy, which is intrinsically linked with its beta-phase nature¹⁵⁴. Similar low strain-hardening behaviour has been reported by researchers focused on the development of other beta-phase alloys^{146,147}, typically in reference to the additional ductility gained as a result. Whilst greater elongation to failure can be beneficial, consideration should be given to its effect on wear degradation and whether such a material will be viable in wear-critical applications (e.g. joint articulating surfaces).

Parallel to development of beta-phase Ti alloys through in-situ alloying, considerable progress has been made in manufacturing alloys where complex geometries are impractical by traditional means, such as NiTi¹⁵⁵ and bulk metallic glasses (BMGs). The amorphous structure of BMGs, which enables low stiffness with up to 50% higher yield strength than Ti-6Al-4V, has been linked to high biocompatibility¹⁵⁶. Given the reduced yield strength seen in beta phase Ti alloys, the enhanced strength of BMGs is appealing. A range of different BMG

compositions have been demonstrated in L-PBF, including Ti-based ¹⁵¹, Fe based ¹⁵⁷, and multiple Zr based alloys ^{148,149}. Further to this, the addition of an amorphous glass fraction to a conventional alloy has been shown using 316L stainless steel and a Fe based BMG ¹⁵⁸. This composite showed improved corrosion resistance, strength and reduced friction versus 316L alone. Critically for clinical application, the use of AM unlocks greater geometric complexity than can be achieved in other BMG manufacturing methods ¹⁵⁹. Highly complex structures with sub-mm features have been produced (Figure 7), demonstrating glassy-lattice structures and sufficient precision to accurately replicate healthy bone geometry.

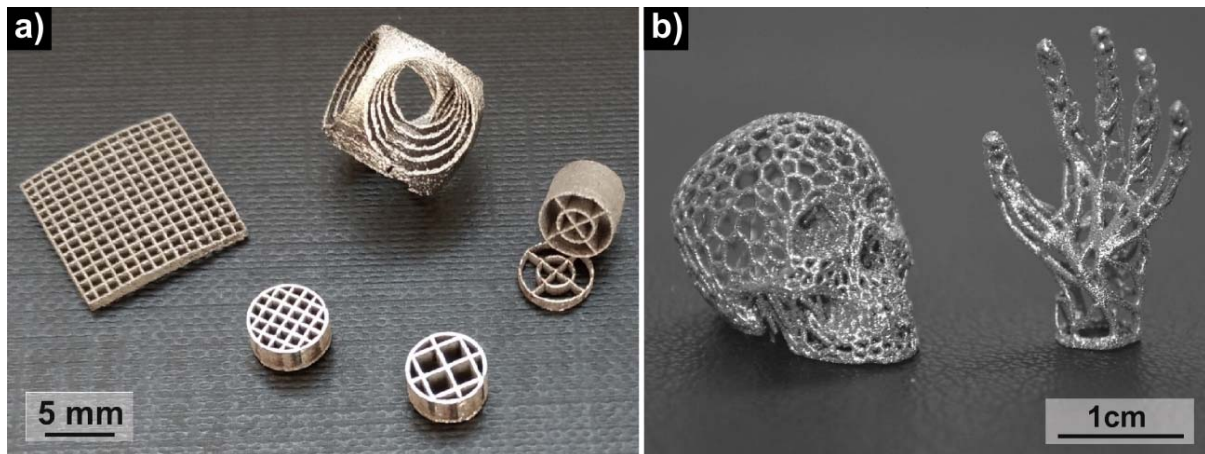


Figure 7 - Bulk metallic glass structures fabricated by L-PBF in a) $Zr_{52.5}Cu_{17.9}Ni_{14.6}Al_{10}Ti_5$ and b) $Ti_{47}Cu_{38}Zr_{7.5}Fe_{2.5}Sn_2Si_1Ag_2$ ^{149,151}

Although BMGs may have a high impact in biomedical applications, there remain significant barriers to their clinical application in the near term (whether manufactured by AM or otherwise). Difficulty in control of porosity, and the trade-off between costly noble metals such as Pd and potentially cytotoxic elements for example Ni and Be, all need to be overcome before translation to *in vivo* models ¹⁵⁶.

3.2.2 Bioactive Alloys

Investigations have been made into alloys that, rather than being effectively inert *in vivo*, exhibit actively osteogenic or antibacterial properties ¹⁶⁰. Particular focus has been on addition of antimicrobial metal ions, such as silver or copper, but experimental materials with integrated hydroxyapatite (HA) have also been demonstrated (Table 3). Note that none of these materials have yet been tested *in vivo* nor, to the best of our knowledge, have any HA containing materials been tested with mammalian tissue cultures.

Table 3 - Examples of additively manufactured bioactive alloys, showing the wide range of base systems and fraction of therapeutic material included.

Active Agent	Base Alloy	Fraction (wt%)	Key Findings	Source
Hydroxy-apatite (HA)	316L steel	5 - 15 vol%	<p>Across all alloys, observe significant reductions in tensile strength and fracture toughness. Associated with porosity and dissolution of P into base alloys.</p> <p>HA acts as a grain refiner, increasing hardness. Increases stiffness in Ti.</p> <p>In Mg-3Zn, see reduced corrosion rate due to protective apatite formation - may also be due to grain refinement.</p>	161 162
	cpTi	2.0 - 5.0		163
		0 - 5.0 gradient		164
	Ti-6Al-7Nb	5.0		165
	NiTi	25		166
	Mg-3Zn	2.5 - 10		167
Cu	316L	4.5	<p>Antimicrobial behaviour increased with aging of alloy, at the cost of lower corrosion resistance. Cytocompatibility demonstrated.</p>	168
		2.5 - 3.5		169
	Ti-6Al-4V	1.38	<p>Efficacy versus E coli and S aureus demonstrated. Observed increase in strength and reduced ductility. Cytocompatibility demonstrated. Addition of Cu encourages differentiation of osteoblasts.</p>	170 135
		5.0		171
		2.0 - 6.0		172 173
	Co-29Cr-9W	3.0	<p>Antimicrobial efficacy demonstrated against E coli and S aureus. Cu increases resistance to corrosion and wear. Cytocompatibility shown.</p>	174 175 176
	ZK60 Mg alloy	0.2 - 0.8	<p>Increased strength, strong antibacterial and cytocompatible.</p>	177
Ag	Ti-6Al-4V	0.5	<p>Dramatically increases ductility, but shows minimal antibacterial behaviour at this level.</p>	171
	ZK30 Mg alloy	0.25 - 1.0	<p>Increased hardness and compressive strength, reduced degradation rate and increased efficacy against <i>E. Coli</i> versus ZK30 alone.</p>	178

Considerable characterisation is needed to find the optimum thermal processing during additive manufacture or heat treatment post-processing, as investigations in non-AM produced antimicrobial alloys have suggested specific metallurgical phases dominate release kinetics¹⁷⁹. Alongside this, further studies are required to establish the optimum loading of therapeutic materials in alloys. Particularly for those alloys that directly incorporate HA, the effect of incorporating additional elements can significantly alter corrosion behaviour, and may override any benefits from improved antimicrobial behaviour or osseointegration.

Given the clear mechanical degradation addition of HA has on composite alloys, a more subtle microalloying approach may prove more mechanically viable in the long-term. Inclusion of key alloying elements to feedstock, such as zirconium to CoCr alloys, has been explored. Using a rabbit femoral model, Zr additions as low as 0.04 wt% increased the torque required to remove implants after eight weeks by 10 %¹⁸⁰. Further histological study of implants in rabbit femur sites showed similar mineral crystallinity, apatite to collagen ratio, and osteocyte density to equivalent CoCr implants after eight weeks¹⁸¹.

Rather than simply encouraging osseointegration, one radical approach to negate mechanical mismatch *in vivo* is the use of bioresorbable Mg, Zn, or Fe alloys, which can be gradually absorbed and replaced by new bone tissue. Clinical trials have shown promising results for the use of Mg in cardiovascular and bone fixation applications, but managing the resorption rate of larger implants is still an open issue^{182–185}. Notably, excessive levels of elements considered ‘biocompatible’ can lead to severe side effects, such as the production of gaseous pockets in the case of Mg^{186,187}. Moreover, changes in geometry of implants as they resorb must be tailored to retain load-bearing requirements. Additively manufactured porous structures may offer a new way to optimise uniformity of degradation, enabling mass transport and allow resorption throughout the volume of an implant (Figure 8), a concept investigated sporadically using non-AM methods¹⁸⁸. The ability to control pore structure via L-PBF has promoted the production of a considerable range of resorbable scaffolds^{189,190}. The effect of porosity on the degradation rate of the Mg alloy WE43 has been demonstrated in depth, with resorption occurring across the entire scaffold and retention of adequate strength and stiffness for 4-weeks *in vitro*¹⁹⁰. In an effort to further optimise degradation kinetics, the use of a polycaprolactone (PCL) coating has been investigated in a mouse calvarial defect model, however the rate of resorption remained sufficiently high that voids were observed between the implant surface and mineralised bone after 84 days¹⁹¹.

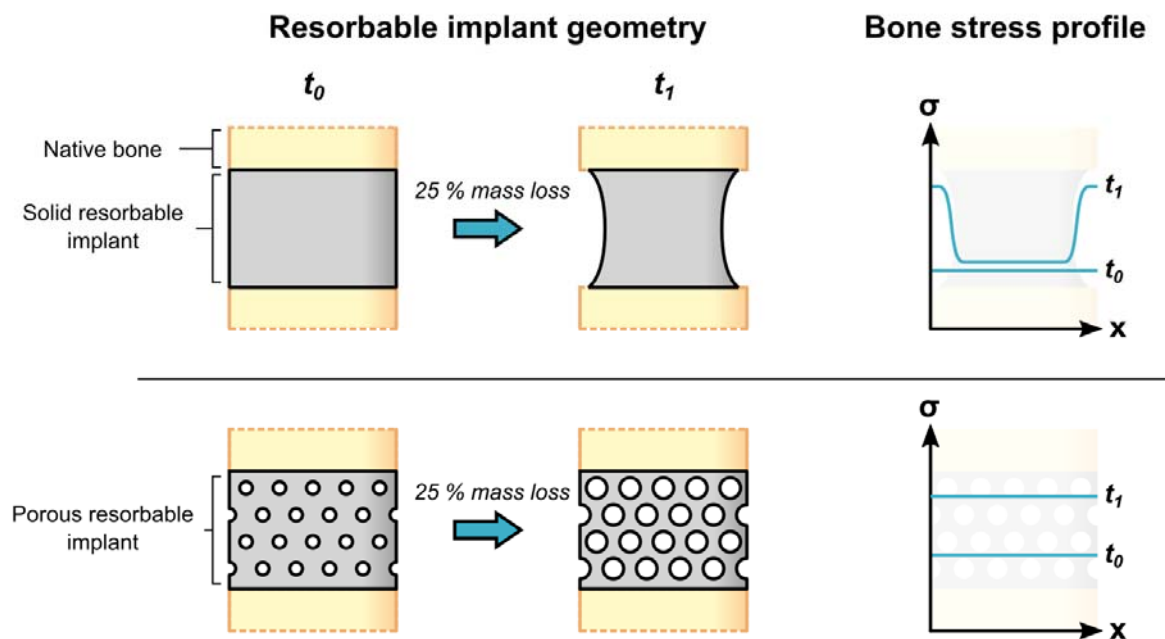


Figure 8 - Schematic showing loading of a resorbable implant under compression, and the resulting change in stress profile of surrounding bone as material resorbs. In a solid implant, the central section of bone continues to suffer from stress shielding, whilst in principle a lattice structure evenly distributes mass loss and load.

Magnesium alloys have been the most widely used resorbable alloys^{192,193}, and as a result a wide range have been processed by L-PBF, including pure Mg, WE43, AZ91 and several Mg-Zn alloys^{167,189,190,194–200}. When produced by conventional means, Mg alloys and particularly pure Mg show low tensile strength, of the order of 30 MPa when cast, requiring heat treatment as a result¹⁹². This may be countered by the fine-grained microstructure AM processes typically produce, whilst concurrently decreasing degradation rate²⁰¹, as has been shown in AZ61 alloy¹⁹⁹. Initial indications of higher micro-hardness of pure Mg versus as-cast are promising in this regard¹⁹⁴. Processing of Mg by L-PBF does nonetheless present challenges, the foremost being the narrow temperature range between melting and boiling points that risks evaporation of material in-process^{196,202}. Similar restrictions in Zn have been managed with in-situ monitoring of melt behaviour²⁰³.

Although no human trials have been carried out on Zn or Fe based degradable implants, they remain a valid option for bioabsorbable implants¹⁸⁷. The ability to process both of these materials has been demonstrated in L-PBF²⁰⁴, with densities in excess of 99 % achievable in Zn^{205,206}. Unlike Mg alloys, Fe based alloys often feature excessively slow degradation due to passivation, a problem that has been combated in L-PBF by addition of silver to optimise corrosion properties²⁰⁷. However, concerns of biocompatibility remain, with 40 times lower daily exposure observed under normal circumstances in comparison to Mg¹⁸⁷. Excess Zn may hinder bone development and at extreme levels causes neurotoxicity, whilst Fe may produce gastrointestinal lesions and liver damage. Further investigation of the alloying content in many Mg alloys is also required, as the toxicity of Yttrium and other rare earth elements found in WE43 alloy is still not well understood²⁰⁸.

4 Challenges of Additive Manufacturing

Whilst there are potential clinical and economic gains to be made from wider use of AM, there are a range of challenges to the reliable manufacture of implants on a mass scale for load-bearing applications. Difficulties can arise both in the initial processing of material, and in the subsequent post-processing of manufactured implants required to achieve optimum mechanical properties.

4.1 Material Processing

As with any manufacturing process, AM processes exhibit unique defects that can be detrimental to mechanical behaviour, and require careful optimisation to avoid. As previously discussed, additively manufactured materials show inherently different microstructural and mechanical behaviours compared to conventional wrought or cast material. High heating and cooling rates result in fine microstructures, whilst the layer-by-layer nature of PBF generates anisotropy and heterogeneous mechanical response. This behaviour is highly process dependent, with a wide range of variables that can be tailored.

Defect generation and techniques for prevention are considered, with a focus on in-process optimisation. Significant work may be required to optimise mechanical properties to meet or exceed those of conventional materials, including the removal of anisotropy. However,

consideration is given to possible functionalisation of material by induced localised anisotropy.

4.1.1 Defect Prevention and Fatigue Behaviour

One of the greatest barriers to wider orthopaedic adoption of AM is a general concern regarding the formation of defects during processing, and particularly their effect on the fatigue strength of AM materials. It has been widely demonstrated that the finer microstructures produced by EB-PBF and L-PBF offer comparable or increased tensile strength to conventionally manufactured equivalents²⁰⁹. However, studies have shown reduced fatigue strength in an as-manufactured state compared to cast or wrought materials in multiple orthopaedic alloys^{210,211}. This is typically ascribed to the high residual stresses in as-manufactured samples, and to a range of process defects as described in Table 4²¹².

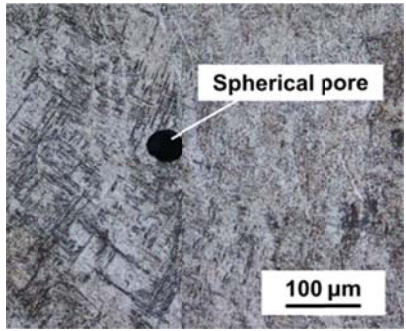
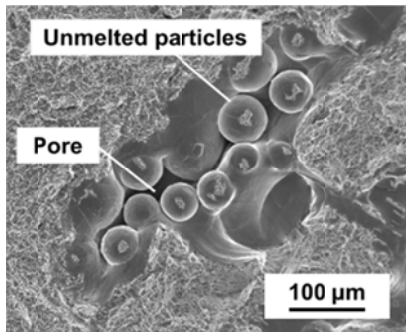
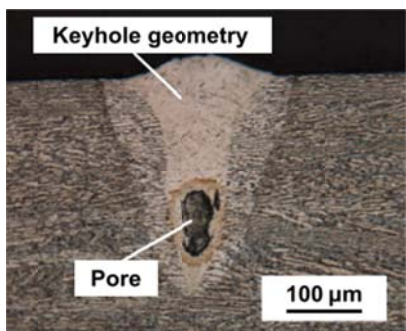
Whilst internal defects may be closed after manufacture by use of hot isostatic pressing (HIPing)²¹¹, so far as reasonably practicable the first recourse should be prevention of defect formation, followed by improvement of post-processing and thermomechanical treatment. Comparisons of Ti-6Al-4V made using different machines and processing parameters has shown that machine-to-machine variability is a significant factor in determining fatigue lifetime²¹³. Regardless of their effect on fatigue, formation of defects indicates a lack of process control that may draw concern from regulators. Complementary advances concerning in-situ process monitoring and metrological inspection methods could translate to improved process reproducibility and stability²¹⁴. In-situ monitoring modules are now available from several key machine manufacturers, that validate the uniformity of powder bed or melt pool characteristics, though data on the improvement in process quality achieved are limited^{215–218}.

Alongside physical modules for optimisation, manufacturers typically provide 'default' parameters with which to produce material – however, significant further optimisation is possible. Starting from the default supplier parameters for Ti-6Al-4V, parametric optimisation has reduced porosity in EB-PBF approximately threefold, with remaining pores ascribed to entrapped gas in feedstock²¹⁹. The cause and morphology of porosity should be considered as well as total volume fraction. In some cases, a trade-off may be made between types of defect, with spherical pores from overmelting in L-PBF as shown by Table 4, considered favourable to elongated voids along build layers²²⁰.

A frequently overlooked aspect of process optimisation for AM is the selection and validation of feedstocks. The majority of materials for powder AM processes are atomised, which can lead to entrapment of gas within powder particles²²¹. Gas atomised powders often show a greater degree of entrapment than those produced using plasma atomisation, with this risk being balanced against a lower cost to manufacture³⁹. A frequent argument for the use of more costly plasma atomised or spheroidised powders is the improved flow properties inherent to a more spherical morphology⁴⁰. However, with appropriate consideration, rough and non-spherical powders have been shown to be processible in EB-PBF²²², and the degree of remnant gas entrapment can be reduced by altering scan strategy to enable gas release²²³. Independent assessment of powder quality should be considered prior to manufacture, including feedstock that is being recycled or reused. Repeated re-use of

powders through PBF processes can be tolerated, though it is common to observe an increase in oxygen content with recycling. Whilst this may reduce ductility, it has been shown that even CoCr powder subjected to deliberate oxidation still produced material within the required standard for cast F75 alloy ²²⁴.

Table 4 - Common internal defects observed in AM parts linked to reduced fatigue strength. Images with publisher's permission from ^{225,226}.

Defect	Cause	Typical Morphology	Image
Pores	Entrapped gas within feedstock powders from atomisation process.	Spherical pores of similar size to feedstock particles.	
Lack of fusion	Incomplete melting of material in process. If consistent across a layer, may lead to delamination due to poor adhesion.	Entrapped unmelted powder feedstock, often in small clusters with surrounding cracks or pores. Frequently observed at fatigue crack surfaces.	
Keyholing	Excessive energy input during processing causing localised vaporisation of material, resulting in pore formation.	Aspherical pore, often surrounded by atypical microstructure in V-shape parallel to build direction.	

4.1.2 Heterogeneous Microstructures

Microstructural heterogeneity and bulk anisotropy are established characteristics of additively manufactured parts. Extreme heating, combined with the layer-wise nature of manufacture, frequently results in elongated grain structures that are heavily dependent on local cooling conditions with typical rates in excess of 10^4 K s^{-1} ^{28,227}. Epitaxial growth of such grains parallel to the build direction is a frequent issue in both laser and electron beam techniques due to remelting of previously deposited material ²²⁸. Such uncontrolled anisotropy causes variation in both tensile and fatigue strength, which must be well understood for any load-bearing application ^{229,230}.

The degree of heterogeneity is highly dependent on process control. Laser power has been shown to have little effect on microstructure scale in L-PBF produced Co-Cr-Mo alloy²³¹, while laser path behaviour altered both dominant crystallographic orientation and extent of columnar grain growth²³². The behaviour of specific phases must also be considered, as investigated in the role of carbide precipitation induced anisotropy in Co-Cr-Mo produced by EB-PBF²³³. There are continuing efforts to optimise process parameters to minimise microstructural heterogeneity, such as in-situ optimisation of Ti-6Al-4V by altering process characteristics. Decreasing the time between melting layers, and increasing layer thickness encourage equiaxed grain formation as opposed to columnar grains, simultaneously increasing ductility by promoting decomposition of martensite²³⁴. Improvements in microstructure have also been shown through a novel approach using a static magnetic field during L-PBF of cp-Ti, reducing the degree of texture observed²³⁵. However, subsequent heat treatment currently remains the most effective method for resolving microstructural variation, adding a costly and time consuming processing step to achieve ideal microstructure and performance¹⁴³.

Despite isotropy of materials being favourable under many circumstances, the material behaviour and stress states of load-bearing bones are complex and anisotropic²³⁶. Cortical bone, for example, exhibits Young's moduli of 20.9 and 11 GPa in the tibia, parallel and perpendicular to the long bone axes respectively¹⁵⁰. Alongside minimisation of anisotropy through optimisation of process control, interest is growing in deliberately producing material inhomogeneity to produce mechanically anisotropic materials²³⁷. The degree of crystallographic anisotropy achievable in a Ni alloy, as shown in Figure 9, is high resulting in stiffness correlating with a basic rule-of-mixtures model²³⁸.

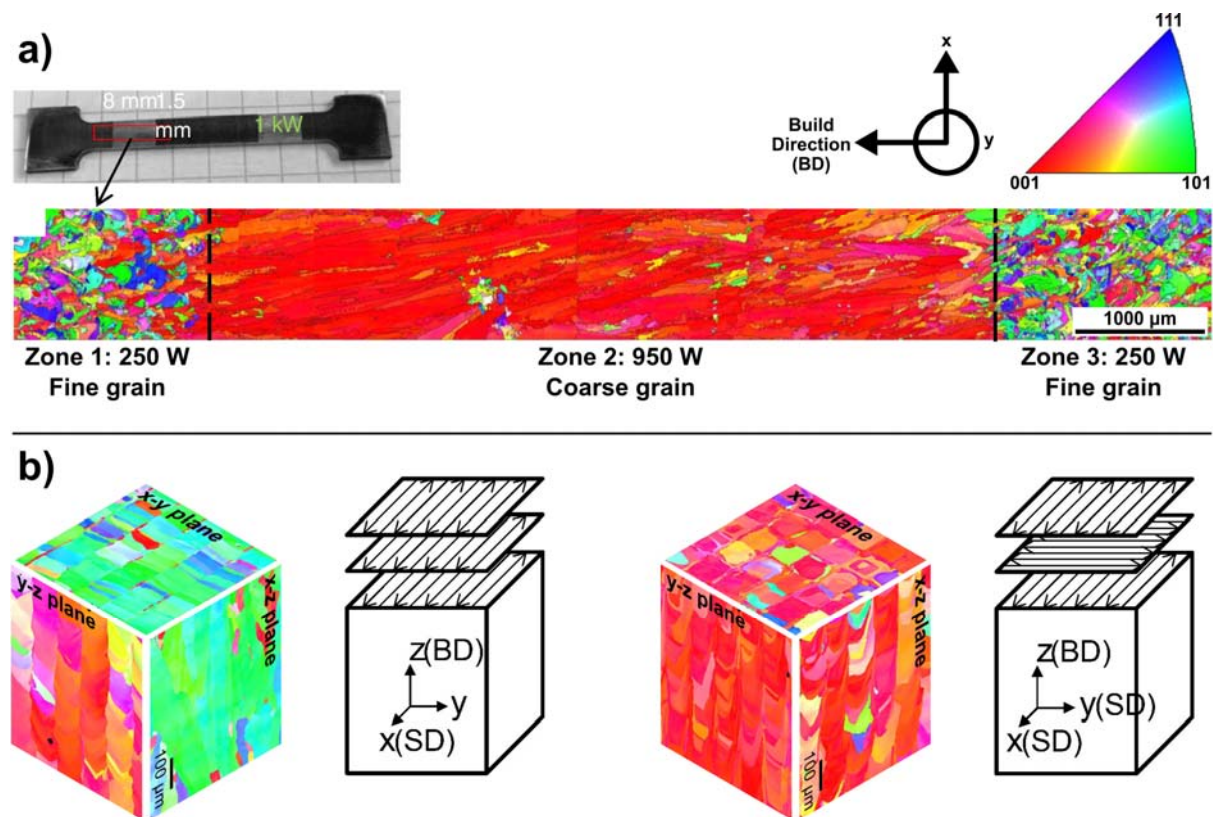


Figure 9 – Electron backscatter diffraction (EBSD) analysis showing the extent of crystalline anisotropy achievable using different laser scanning parameters during L-PBF. The index map shown at top right applies to both a) a transition between fine, randomly oriented grains and coarse, aligned grains in Inconel-718 by altering power, and b) tailoring of grain orientation in a Ti alloy by changing the scan direction (SD) of alternating layers.^{238,239}

No functional grading has yet been demonstrated along the X-Y plane of biomedical alloys within a single component. However, alternating layers of microstructures have been produced in a NiTi shape memory alloy, with alternate austenitic and martensitic structures inducing the Elinvar effect, where the temperature dependence of stiffness is negligible²⁴⁰. A similar high degree of microstructural control has been demonstrated over low modulus Ti-15Mo-5Zr-3Al alloy, preferentially generating either <001> and <011> orientations along the build direction²³⁹.

4.2 Post-Process Optimisation

Whilst the ease of access to AM technologies continues to increase, it remains the case that metal powder technologies are far from a ‘press-play’ solution. The surface finish and mechanical properties of parts in the ‘as-built’ state can be significantly improved upon with appropriate post manufacture processing. The application of conventional surface finishing techniques to AM implants is non-trivial for several reasons;

1. Novel implant geometries, including porous scaffold or lattice type structures, which preclude the use of many line-of-sight techniques.
2. Specific initial surface finish of AM implants, including partially adhered powder feedstock and variable roughness with orientation.
3. Possible needs for variable finish across implants (e.g. roughened outer surface of acetabular cups for osseointegration vs polished interior articulating face).

These same complications may clash with existing coating techniques such as plasma spraying or sputtering, which are frequently used to add functionality, particularly in orthopaedics.

Alongside surface finishing, thermal processing is a key consideration to optimise microstructure and reduce the risk of fatigue induced failure. As such in this section, the state of the art in both surface and thermal processing is covered.

4.2.1 Surface Processing

Conventional surface processing techniques used for biomedical implants face severe challenges when applied to AM structures. For example, sand-blasting followed by acid etching (SLA - Sand-blasted, Large grit, Acid etched) is a common surface finishing technique used to induce multi-scale roughness, both on commercial implants and in a laboratory setting^{241,242}. However, its high directionality makes it inappropriate for the finishing of complex geometries or lattices²⁴³, and the existing roughness of as-built AM surfaces may encourage entrapment of remnant grit, with a detrimental effect on biocompatibility and increased risk of bacterial colonisation²⁴⁴. Several commercially available implants utilise designed porosity, such as acetabular cups, and whilst bearing

surfaces are machined smooth, removal of remnant powder from the porous surface is a key consideration. Ultrasonic cleaning is often raised as an option, however may be insufficient to remove all remnant particulate matter²⁴⁵, and will do little to remove surface defects common to AM parts that reduce fatigue strength²⁴⁶.

To cope with complex geometry, liquid-phase techniques offer a way to access all exposed surfaces. In non-medical fields, interest has focussed on use of abrasive flow machining (AFM) and its derivatives, in which a suspension of abrasive media is forced through a vessel containing the specimen to be polished. The viability of hybrid chemical-abrasive flow techniques for internal channels has been verified for additively manufactured specimens²⁴⁷, whilst ultrasonic cavitation abrasive finishing (UCAF) also showed promise using a range of abrasive concentrations, including cavitation with no abrasive²⁴⁸. Translation of these technologies to a medical field would require careful consideration of toxicity of the etchants or abrasives used while still considering the risk of remnant media.

In order to avoid any form of remnant media, various chemical polishing processes - referred to in terms of etching or passivation depending on the effect on surface oxide state - have been used on bulk and lattice structures. A mixed acid polish using nitric and hydrofluoric acids removed a significant proportion of adhered powder from the L-PBF process²⁴⁹, and also reduced *S. Aureus* biofilm formation on Ti-6Al-7Nb lattices compared to ultrasonic cleaning alone¹³⁹. From an osseointegrative perspective, alkaline etching of commercially pure Ti with a mix of NH₄OH/H₂O₂ boosted proliferation of MG-63 cells²⁵⁰. However, such chemically aggressive processes may have negative effects on a part's strength, with significant mass loss in lattice structures due to the high surface to volume ratio (Figure 10). Excess material removal can significantly reduce fatigue strength as demonstrated in Acid-Alkali treatments of Ti-6Al-4V²⁵¹, negating the benefits typically seen from removing surface defects or remnant media²⁵². Allowances for the reduction in volume must be included at a design stage to compensate once appropriate analysis of mass and volume loss has been made, as has been demonstrated for existing liquid phase techniques, such as electropolishing²⁵³.

As well as modifying roughness, these processes may alter the chemical composition of the surface, through deposition of remnant abrasive²⁴⁴, or modification of oxide layers²⁵¹. It is important to consider the effect of any post processing on oxide behaviour, as the extent and morphology of oxide film growth can be controlled²⁵⁴. Notably, both thickness²⁵⁵ and microstructure of the oxide layer can alter cell response²⁵⁶.

A final aspect of surface processing to consider is the well-established use of coatings to generate combination products capable of delivering therapeutic agents^{257–261}. The fundamental principles of these technologies are generally not expected to behave differently on AM materials to conventionally manufactured implants due to nominally identical chemistries. However, there has been relatively little consideration of how to adapt coatings for the complex scaffolds or porous structures possible with L-PBF and EB-PBF. As with surface finishing, liquid or gas phase processes show the greatest promise to adequately deal with such complex geometries, with Yavari *et al* demonstrating the doping of titanium scaffolds with silver ions for antimicrobial effect²⁶², and multiple papers reporting liquid-phase approaches to coat lattices with a range of hydroxyapatite derivatives^{263–266}, silicates²⁶⁶, and collagen²⁶⁷. On the other hand, discussion of coverage quality achieved is

rare. When investigated, poor uniformity across the internal structures of lattices is noted, for example in the integration of poly- ϵ -caprolactone and poly(3-hydroxybutyrate) ¹⁹¹.

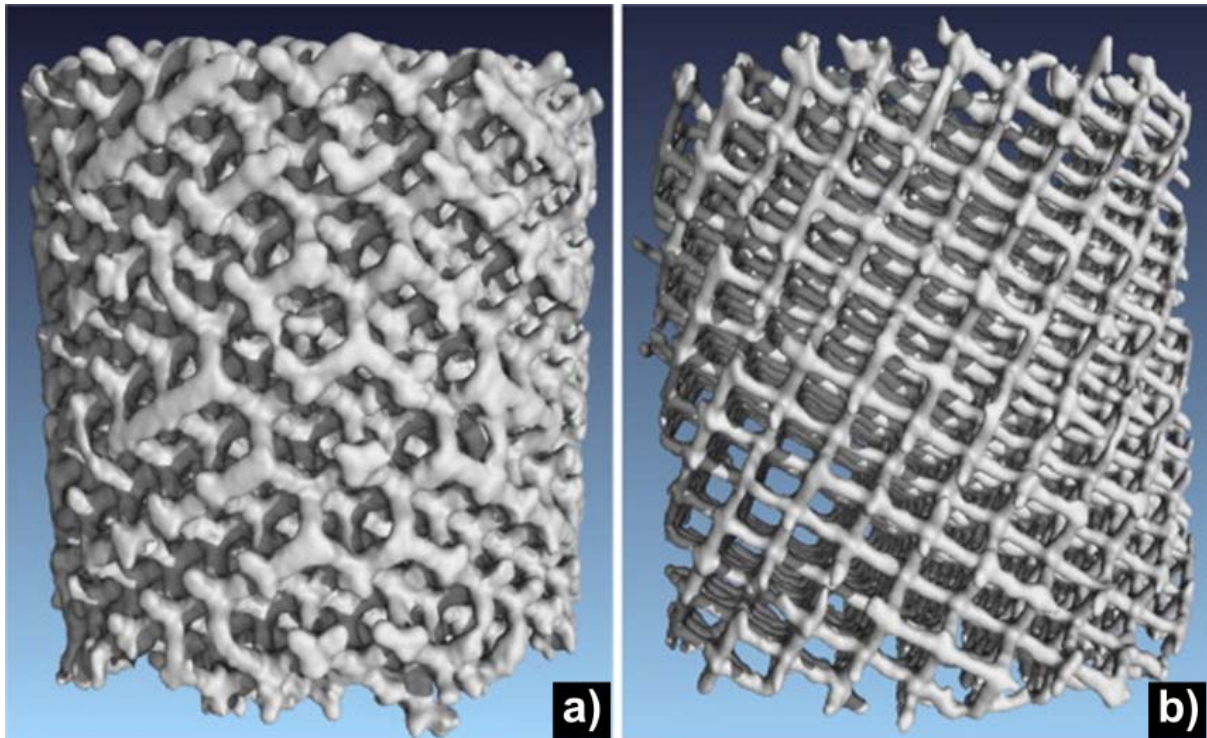


Figure 10 - Reconstructions of micro X-ray computed tomography scans of a Ti-6Al-7Nb lattice structure a) before and b) after chemical etching with aqueous 6 vol% HF and 14 vol% HNO₃ for 600 seconds. Note the visible decrease in volume. ²⁴⁹

Given the challenges related to coating AM parts, even in liquid phase, significant further thought needs to be given to whether there remains utility in line-of-sight techniques, such as plasma-spraying or physical vapour deposition in combination with complex geometry ²⁶⁸. Moreover, it is worth a measure of caution in the use or reliance upon novel coating technologies, as whilst there are a range of orthopaedic coatings approved for use, a large proportion of developed surface coatings remain in a pre-clinical phase ²⁶¹. Though aligning development of novel AM implants and related coatings may provide a leap in theoretical clinical benefit, critical assessment of the viability to combine them is necessary.

4.2.2 Thermal Post Processing for Fatigue

Whilst bulk defects should be minimised in-process, the inherent limitations of AM processes necessitate a degree of post-processing to obtain optimal fatigue performance. It is important to note that, provided appropriate process control and post-processing is applied, AM materials do not inherently show poorer fatigue performance than conventional materials. Comprehensive study of literature for AM Ti-6Al-4V by Li et al has shown that combining surface finishing and heat treatment, fatigue performance even exceeds cast and wrought material ²⁶⁹.

That being said, the as-built state of AM parts can be challenging, with surface texture acting as nucleation sites for fatigue cracking ²⁷⁰, whilst residual thermal stresses or sub-optimal microstructures can reduce fatigue lifetimes ²⁷¹. Where possible, machining or polishing can

dramatically increase fatigue lifetime by removal of surface defects²⁷². If internal defects occur, HIPing is currently the only viable post-process technique to close defects. It is important to consider the alloy specific requirements of any heat treatment, and there have been extensive studies on the effects of HIPing in Ti-6Al-4V due to its frequent use in non-biomedical contexts^{212,273–276}. HIPing has been shown to increase fatigue lifetime²⁷⁵, but there is evidence that it has negligible effect on fatigue strength when variable amplitude loading is considered²⁷⁶. This is crucial to orthopaedic settings, as variable loading is typical during walking and is observed in orthopaedic models²⁷⁷. There are fewer studies of CoCr based alloys, though similar improvements in fatigue strength from the as built state are observed following HIPing²¹¹. In all alloys, care must be taken where pores are introduced by entrapped gas within atomised powder feedstocks, as subsequent heat treatment may reopen pores initially closed by HIPing²⁷⁸.

Efforts have been made to negate the need for post-process heat treatment, particularly with respect to residual stresses induced by high thermal gradients during processing. Careful optimisation of scanning parameters can reduce thermal gradient, leading to, in one case, a reduction in thermal deformation of 36 %, though this is significantly less than the 80 % reduction achieved through heat treatment²⁷⁹. Maintaining an elevated chamber temperature during manufacture as in EB-PBF and certain hot-bed L-PBF setups can provide some stress relief^{280–282}, but heat treatment remains the most easily accessible and optimal method for improving fatigue strength.

Further work is also necessary to develop models of fatigue behaviour for AM materials, particularly lattices which are especially prone to fatigue, exhibiting lower normalised fatigue endurance limits than solid material²⁸³. Multiscale techniques show promise by considering a microscale model at a crack tip, whilst simplifying to a macroscopic model of stress distribution further from the tip²⁸⁴, but may be difficult to apply to complex implant geometries. In practice, a combination of etching to remove surface defects, and HIPing to minimise internal defects and provide heat treatment, has been identified as an optimal method for improving Ti-6Al-4V lattice fatigue lifetimes, particularly in the high cycle regime²⁵². Similar chemical etching has also shown promise in CoCr F75 alloy, with performance under quasi-static fatigue retained²⁸⁵, though the effect of thermal processing requires further study.

5 Regulatory Challenges

As with any new medical device, compliance with regulation to ensure patient safety must be considered well in advance of submission to regulatory bodies. Within the Europe Union, the ongoing transition from the Medical Devices Directive (93/42/EEC) and Active Implantable Medical Devices Directive (90/385/EEC) to the Medical Devices Regulation (Regulation (EU) 2017/745) or 'MDR' has increased both awareness and scrutiny of implantable devices⁴⁶. As discussed in Section 2, the current approach to implant manufacture can be broadly segregated into two groups;

1. Patient-specific or “custom” devices where no alternative implant exists, whose use can be justified through last resort where the benefits outweigh the risks of a novel device
2. More typical mass-manufactured implants that must be proven to meet or exceed performance of existing devices

The need to prove equivalent performance to existing implants is especially true in the case of ‘active’ implants, i.e. those with load bearing and articulating behaviours as in orthopaedics. Whilst this is not an unfamiliar regulatory barrier when considering new design geometries, it is in proving equivalent performance of materials that AM faces significant barriers. Current materials used, such as cast or wrought Ti-6Al-4V, Co-Cr, or 316L steel, are considered well-characterised, with understood behaviours over periods of 10 to 15 years *in vivo*. Materials produced by AM, regardless of equivalence of composition, are not yet at this stage of well-characterised behaviour, and as discussed in Section 4.1.1, frequently show different failure behaviour²¹⁰. As such, a significant burden of proof will lie in proving either direct equivalence of behaviour, or appropriate consideration and investigation to mitigate risk. Note also the extended period of behaviour that must be considered, with the need to ‘*identify and analyse the known and foreseeable hazards associated with each device*’ (MDR Annex I, Chapter 1, 3(a).)⁴⁶. Within the context of the MDR, demonstration of equivalence to an implant also relies upon access to data generated during validation of said implant. If this has been produced by another manufacturer, unless the data generated has been published, accessing such confidential information may prove challenging to new manufacturers entering the market.

Considering the L-PBF or EB-PBF processes in more detail, control and traceability of powder feedstocks is one example of the process-specific challenges present. Manufacturers of feedstock will come under increasing pressure to demonstrate provenance of the material entering atomisers, guaranteeing only single alloys have been used and ensuring the quality of resulting powders. Several large powder suppliers have achieved ISO 13485 to supply for medical applications, and proof of compliance with this and future standards will remain critical as AM production becomes more common^{286,287}. Once obtained, feedstocks need to be appropriately validated, and whilst guiding standards such as ASTM F3049-14 exist there is as yet no harmonised standard suite of characterisation processes that should be applied as a minimum, even if there are standards for individual tests²⁸⁸. Beyond initial characterisation, the common practise of reusing or ‘recycling’ powder that has not been melted during the process will require justification, with validation that any shifts in size distribution and oxygen content are acceptable^{289,290}. The physical manufacturing process must also be standardised for each approved device, and the exact process parameters used justified to the notified body. Scanning and melt parameters as well as tolerances, and acceptable deviations in part dimensions are all aspects that should be considered. This presents an opportunity for a leading supplier to establish a standard for others to follow, as currently there are no harmonised standards relating to process parameters, merely mechanical behaviour of produced material.

The burden of proof lies with the manufacturer to prove the device performs as well as or better than existing approved implants; above all, every step of the manufacturing process from feedstock to sterilisation must be appropriately considered, justified, and validated. Validation of work conducted for the compilation of a pre-market technical dossier must be

conducted in line with current standards - particularly harmonised EN ISO standards where possible - or if appropriate standards do not exist, following engineering or scientific state of the art. Given the broader push for standard development across the AM sector, it remains in the interest of medical device manufacturers to be involved in this process and drive standards in a useful direction.

6 Conclusions

Across researchers, manufacturers, regulators, and clinicians, AM presents opportunities for new approaches. Though data for long-term outcomes remain limited, additive manufacturing of metallic implants has shown clear benefits in application to patient specific implants. Assessing a case study of cranioplasty manufacture, the additional design flexibility offered and greater feedback possible between clinicians and prosthetists provides a model for broader adoption.

There are a number of advances being made in laboratory settings that show promise for translation, which have been discussed with specific clinical targets in mind. The added flexibility of design and material possible through AM show particular promise to reduce stress shielding, a major factor in revisions due to aseptic loosening. With that in mind, it is critical for researchers to consider the viability of bringing such advances into clinical practice. Several challenges remain to widening the use of AM implants, particularly in guaranteeing the consistency of material produced and its optimum performance.

It is crucial that the full path to translation is considered during research, including the long-term goal of clinical use. Considering the current regulatory framework for implantable devices, there are challenges to meeting the high specification needed for orthopaedic application. Equally, as AM becomes more widely used, it may be necessary to reassess the regulatory position on the breadth of 'design envelope' that covers mass manufactured implants.

References

1. NJR. 14th Annual Report National Joint Registry for England, Wales, Northern Ireland and the Isle of Man. *Natl. Jt. Regist.* (2017).
2. Scottish Arthroplasty Project. *Scottish Arthroplasty Project Annual Report 2017*. (2017).
3. Health and Social Care Information Centre. *Hospital Admitted Patient Care Activity*. (2018).
4. OECD Publishing. Hip and knee replacement. in *Health at a Glance 2017* (OECD, 2017). doi:10.1787/health_glance-2017-en 10.1787/health_glance-2017-en
5. OECD. *OECD Labour Force Statistics*. (OECD, 2018). doi:10.1787/oecd_lfs-2017-en 10.1787/oecd_lfs-2017-en
6. Kurtz, S., Ong, K., Lau, E., Mowat, F. & Halpern, M. Projections of Primary and Revision Hip and Knee Arthroplasty in the United States from 2005 to 2030. *J. Bone Jt. Surg.* **89**, 780 (2007). 10.2106/JBJS.F.00222
7. Pilz, V., Hanstein, T. & Skripitz, R. Projections of primary hip arthroplasty in Germany until 2040. *Acta Orthop.* **89**, 308–313 (2018). 10.1080/17453674.2018.1446463
8. Culliford, D. *et al.* Future projections of total hip and knee arthroplasty in the UK: results from the UK Clinical Practice Research Datalink. *Osteoarthr. Cartil.* **23**, 594–600 (2015). 10.1016/J.JOCA.2014.12.022
9. Zimmerli, W. & Ochsner, P. E. Management of Infection Associated with Prosthetic Joints. *Infection* **31**, 99–108 (2003). 10.1007/s15010-002-3079-9
10. Chikuda, H. *et al.* Impact of age and comorbidity burden on mortality and major complications in older adults undergoing orthopaedic surgery: an analysis using the Japanese diagnosis procedure combination database. *BMC Musculoskelet. Disord.* **14**, 173 (2013). 10.1186/1471-2474-14-173
11. Farrar, N., Alaker, M. & Duckett, S. A cost analysis of elective hip revision arthroplasty versus periprosthetic hip fracture management in a district general hospital. *Bull. R. Coll. Surg. Engl.* **97**, E26–E29 (2015). 10.1308/147363515X14134529302506
12. Klouche, S., Sariali, E. & Mamoudy, P. Total hip arthroplasty revision due to infection: A cost analysis approach. *Orthop. Traumatol. Surg. Res.* **96**, 124–132 (2010). 10.1016/J.OTSR.2009.11.004
13. Alp, E., Cevahir, F., Ersoy, S. & Guney, A. Incidence and economic burden of prosthetic joint infections in a university hospital: A report from a middle-income country. *J. Infect. Public Health* **9**, 494–498 (2016). 10.1016/J.JIPH.2015.12.014
14. Rack, H. J. & Qazi, J. I. Titanium alloys for biomedical applications. *Mater. Sci. Eng. C* **26**, 1269–1277 (2006). 10.1016/J.MSEC.2005.08.032
15. Milošev, I. *Biomedical Applications*. **55**, (Springer US, 2012). 10.1007/978-1-4614-3125-1
16. van Lenthe, G. H., de Waal Malefijt, M. C. & Huiskes, R. Stress Shielding After Total Knee Replacement May Cause Bone Resorption In The Distal Femur. *J. Bone Jt. Surg.* **79**, 117–122 (1997). 10.1016/0040-1951(81)90193-1
17. Goriainov, V., Cook, R., M. Latham, J., G. Dunlop, D. & Oreffo, R. O. C. Bone and metal: An orthopaedic perspective on osseointegration of metals. *Acta Biomater.* **10**, 4043–4057 (2014). 10.1016/j.actbio.2014.06.004
18. Australian Orthopaedic Association. *Hip, Knee & Shoulder Arthroplasty: 2017 Annual Report*. (2017).
19. Gittens, R. A. *et al.* The roles of titanium surface micro/nanotopography and wettability on the differential response of human osteoblast lineage cells. *Acta Biomater.* **9**, 6268–6277 (2013). 10.1016/J.ACTBIO.2012.12.002
20. Wu, Y., Zitelli, J. P., TenHuisen, K. S., Yu, X. & Libera, M. R. Differential response of Staphylococci and osteoblasts to varying titanium surface roughness. *Biomaterials* **32**, 951–960 (2011). 10.1016/j.biomaterials.2010.10.001
21. Le Guehennec, L. *et al.* Osteoblastic cell behaviour on different titanium implant

- surfaces. *Acta Biomater.* **4**, 535–543 (2008). 10.1016/j.actbio.2007.12.002
22. Lincks, J. *et al.* Response of MG63 osteoblast-like cells to titanium and titanium alloy is dependent on surface roughness and composition. *Biomaterials* **19**, 2219–2232 (1998).
23. Williams, L. R., Fan, K. F. & Bentley, R. P. Custom-made titanium cranioplasty: early and late complications of 151 cranioplasties and review of the literature. *Int. J. Oral Maxillofac. Surg.* **44**, 599–608 (2015). 10.1016/j.ijom.2014.09.006
24. Arciola, C. R., Campoccia, D. & Montanaro, L. Implant infections: adhesion, biofilm formation and immune evasion. *Nat. Rev. Microbiol.* **16**, 397–409 (2018). 10.1038/s41579-018-0019-y
25. Stewart, P. S. & William Costerton, J. Antibiotic resistance of bacteria in biofilms. *Lancet* **358**, 135–138 (2001). 10.1016/S0140-6736(01)05321-1
26. ASTM ISO/ASTM52900-15 Standard Terminology for Additive Manufacturing – General Principles – Terminology. (2015).
27. Cao, F., Zhang, T., Ryder, M. A. & Lados, D. A. A Review of the Fatigue Properties of Additively Manufactured Ti-6Al-4V. *JOM* **70**, 349–357 (2018). 10.1007/s11837-017-2728-5
28. Herzog, D., Seyda, V., Wycisk, E. & Emmelmann, C. Additive manufacturing of metals. *Acta Mater.* **117**, 371–392 (2016). 10.1016/J.ACTAMAT.2016.07.019
29. Gorse, S., Hutchinson, C., Gouné, M. & Banerjee, R. Additive manufacturing of metals: a brief review of the characteristic microstructures and properties of steels, Ti-6Al-4V and high-entropy alloys. *Sci. Technol. Adv. Mater.* **18**, 584–610 (2017). 10.1080/14686996.2017.1361305
30. Hussein, M., Mohammed, A. & Al-Aqeeli, N. Wear Characteristics of Metallic Biomaterials: A Review. *Materials (Basel)*. **8**, 2749–2768 (2015). 10.3390/ma8052749
31. Perticarini, L., Zanon, G., Rossi, S. M. P. & Benazzo, F. M. Clinical and radiographic outcomes of a trabecular titaniumTM acetabular component in hip arthroplasty: results at minimum 5 years follow-up. *BMC Musculoskelet. Disord.* **16**, 375 (2015). 10.1186/s12891-015-0822-9
32. Learmonth, I. D., Young, C. & Rorabeck, C. The operation of the century: total hip replacement. *Lancet* **370**, 1508–1519 (2007). 10.1016/S0140-6736(07)60457-7
33. McMinn, D. *Modern Hip Resurfacing. Modern Hip Resurfacing* (Springer, 2009). doi:10.1007/978-1-84800-088-9 10.1007/978-1-84800-088-9
34. K2M. Lamellar 3D Titanium Technology. *Platform Technologies - Information Page* (2015). Available at: <http://www.k2m.com/platform-technologies/technology/lamellar-titanium-technology/>. (Accessed: 4th October 2018)
35. 4WEB Medical. Osteotomy Truss SystemTM – Evans : 4WEB Medical. Available at: <https://4webmedical.com/products/osteotomy-truss-system-evans/>. (Accessed: 4th October 2018)
36. U.S. Food and Drug Administration (FDA). 510(k) Premarket Notification Database. (2019). Available at: <https://www.accessdata.fda.gov/scripts/cdrh/cfdocs/cfPMN/pmn.cfm>. (Accessed: 3rd May 2019)
37. Ford, S. & Despeisse, M. Additive manufacturing and sustainability: an exploratory study of the advantages and challenges. *J. Clean. Prod.* **137**, 1573–1587 (2016). 10.1016/J.JCLEPRO.2016.04.150
38. Luo, W. *et al.* Customized Knee Prosthesis in Treatment of Giant Cell Tumors of the Proximal Tibia: Application of 3-Dimensional Printing Technology in Surgical Design. *Med. Sci. Monit.* **23**, 1691–1700 (2017). 10.12659/MSM.901436
39. Dawes, J., Bowerman, R. & Trepleton, R. Introduction to the Additive Manufacturing Powder Metallurgy Supply Chain. *Johnson Matthey Technol. Rev.* **59**, 243–256 (2015). 10.1595/205651315X688686
40. Sun, P., Fang, Z. Z., Zhang, Y. & Xia, Y. Review of the Methods for Production of Spherical Ti and Ti Alloy Powder. *JOM* **69**, 1853–1860 (2017). 10.1007/s11837-017-2513-5

41. Weller, C., Kleer, R. & Piller, F. T. Economic implications of 3D printing: Market structure models in light of additive manufacturing revisited. *Int. J. Prod. Econ.* **164**, 43–56 (2015). 10.1016/J.IJPE.2015.02.020
42. Elbuluk, A. M., Old, A. B., Bosco, J. A., Schwarzkopf, R. & Iorio, R. Strategies for reducing implant costs in the revision total knee arthroplasty episode of care. *Arthroplast. Today* **3**, 286–288 (2017). 10.1016/J.ARTD.2017.03.004
43. Dawood, A., Marti, B. M., Sauret-Jackson, V. & Darwood, A. 3D printing in dentistry. *Br. Dent. J.* **219**, 521–529 (2015). 10.1038/sj.bdj.2015.914
44. Kassapidou, M., Franke Stenport, V., Hjalmarsson, L. & Johansson, C. B. Cobalt-chromium alloys in fixed prosthodontics in Sweden. *Acta Biomater. Odontol. Scand.* **3**, 53–62 (2017). 10.1080/23337931.2017.1360776
45. Di Prima, M. *et al.* Additively manufactured medical products – the FDA perspective. *3D Print. Med.* **2**, 1 (2015). 10.1186/s41205-016-0005-9
46. European Commission. *REGULATION (EU) 2017/745 OF THE EUROPEAN PARLIAMENT AND OF THE COUNCIL of 5 April 2017 on medical devices, amending Directive 2001/83/EC, Regulation (EC) No 178/2002 and Regulation (EC) No 1223/2009 and repealing Council Directives 90/385/EEC and 93/42/EE.* *Official Journal of the European Union* **60**, 2–175 (European Parliament, 2017).
47. Giese, H. *et al.* German Cranial Reconstruction Registry (GCRR): protocol for a prospective, multicentre, open registry. *BMJ Open* **5**, e009273 (2015). 10.1136/bmjopen-2015-009273
48. Koliass, A. G. *et al.* Proposal for establishment of the UK Cranial Reconstruction Registry (UKCRR). *Br. J. Neurosurg.* **28**, 310–314 (2014). 10.3109/02688697.2013.859657
49. Renishaw. Digital evolution of cranial surgery. (2017). Available at: <http://www.renishaw.com/en/digital-evolution-of-cranial-surgery--38602>. (Accessed: 4th October 2018)
50. TCT Magazine. CEIT Biomedical Engineering gets EU approval for 3D printed cranial implants - TCT Magazine. *TCT Magazine* (2014). Available at: <https://www.tctmagazine.com/3d-printing-news/eu-approval-for-3d-printed-cranial-implants/>. (Accessed: 4th October 2018)
51. Laser Systems Europe. Titanium 3D printed implants transform craniomaxillofacial surgery. *Laser Systems Europe* (2017). Available at: <https://www.lasersystemseurope.com/news/titanium-3d-printed-implants-transform-craniomaxillofacial-surgery>. (Accessed: 4th October 2018)
52. Fan, H. *et al.* Implantation of customized 3-D printed titanium prosthesis in limb salvage surgery: a case series and review of the literature. *World J. Surg. Oncol.* **13**, 308 (2015). 10.1186/s12957-015-0723-2
53. Lu, M. *et al.* Uncemented three-dimensional-printed prosthetic reconstruction for massive bone defects of the proximal tibia. *World J. Surg. Oncol.* **16**, 47 (2018). 10.1186/s12957-018-1333-6
54. Rotaru, H., Schumacher, R., Kim, S.-G. & Dinu, C. Selective laser melted titanium implants: a new technique for the reconstruction of extensive zygomatic complex defects. *Maxillofac. Plast. Reconstr. Surg.* **37**, 1 (2015). 10.1186/s40902-015-0001-9
55. Tam, M. D., Laycock, S. D., Bell, D. & Chojnowski, A. 3-D printout of a DICOM file to aid surgical planning in a 6 year old patient with a large scapular osteochondroma complicating congenital diaphyseal aclasia. *J. Radiol. Case Rep.* **6**, 31–7 (2012). 10.3941/jrcr.v6i1.889
56. Honeybul, S., Morrison, D. A., Ho, K. M., Lind, C. R. P. & Geelhoed, E. A randomized controlled trial comparing autologous cranioplasty with custom-made titanium cranioplasty. *J. Neurosurg.* **126**, 81–90 (2017). 10.3171/2015.12.JNS152004
57. Andrabai, S., Sarmast, A., Kirmani, A. & Bhat, A. Cranioplasty: Indications, procedures, and outcome – An institutional experience. *Surg. Neurol. Int.* **8**, 91 (2017). 10.4103/sni.sni_45_17
58. Vahntsevanos, K. *et al.* The Atkinson Morley's Hospital joint neurosurgical –

- maxillofacial procedures: Cranioplasty case series 1985–2003. *J. Cranio-Maxillofacial Surg.* **35**, 336–342 (2007). 10.1016/J.JCMS.2007.06.002
59. Mukherjee, S., Thakur, B., Haq, I., Hettige, S. & Martin, A. J. Complications of titanium cranioplasty—a retrospective analysis of 174 patients. *Acta Neurochir. (Wien)*. **156**, 989–998 (2014). 10.1007/s00701-014-2024-x
 60. Tasiou, A. *et al.* Cranioplasty optimal timing in cases of decompressive craniectomy after severe head injury: a systematic literature review. *Interdiscip. Neurosurg.* **1**, 107–111 (2014). 10.1016/J.INAT.2014.06.005
 61. Thavarajah, D., Lacy, P. De, Hussien, A. & Sugar, A. The minimum time for cranioplasty insertion from craniectomy is six months to reduce risk of infection- a case series of 82 patients. *Br. J. Neurosurg.* **26**, 78–80 (2012). 10.3109/02688697.2011.603850
 62. Bender, A. *et al.* Early cranioplasty may improve outcome in neurological patients with decompressive craniectomy. *Brain Inj.* **27**, 1073–1079 (2013). 10.3109/02699052.2013.794972
 63. Wachter, D., Reineke, K., Behm, T. & Rohde, V. Cranioplasty after decompressive hemicraniectomy: Underestimated surgery-associated complications? *Clin. Neurol. Neurosurg.* **115**, 1293–1297 (2013). 10.1016/J.CLINURO.2012.12.002
 64. Renishaw. LaserImplant - case timeline (UK only). (2016). Available at: <http://www.renishaw.com/go/media/pdf/en/3dcb96b444bf4ad6aed3394b779943ec.pdf> . (Accessed: 9th April 2018)
 65. Oettmeier, K. & Hofmann, E. Impact of additive manufacturing technology adoption on supply chain management processes and components. *J. Manuf. Technol. Manag.* **27**, 944–968 (2016). 10.1108/JMTM-12-2015-0113
 66. Huang, S. H., Liu, P., Mokasdar, A. & Hou, L. Additive manufacturing and its societal impact: a literature review. *Int. J. Adv. Manuf. Technol.* **67**, 1191–1203 (2013). 10.1007/s00170-012-4558-5
 67. Peel, S., Eggbeer, D., Burton, H., Hanson, H. & Evans, P. L. Additively manufactured versus conventionally pressed cranioplasty implants: An accuracy comparison. *Proc. Inst. Mech. Eng. Part H J. Eng. Med.* **232**, 949–961 (2018). 10.1177/0954411918794718
 68. Lee, C.-H., Chung, Y. S., Lee, S. H., Yang, H.-J. & Son, Y.-J. Analysis of the factors influencing bone graft infection after cranioplasty. *J. Trauma Acute Care Surg.* **73**, 255–260 (2012). 10.1097/TA.0b013e318256a150
 69. Jackson, T. D., Wannares, J. J., Lancaster, R. T., Rattner, D. W. & Hutter, M. M. Does speed matter? The impact of operative time on outcome in laparoscopic surgery. *Surg. Endosc.* **25**, 2288–95 (2011). 10.1007/s00464-010-1550-8
 70. Phan, K. *et al.* Anesthesia Duration as an Independent Risk Factor for Early Postoperative Complications in Adults Undergoing Elective ACDF. *Glob. spine J.* **7**, 727–734 (2017). 10.1177/2192568217701105
 71. Thomas-Seale, L. E. J., Kirkman-Brown, J. C., Attallah, M. M., Espino, D. M. & Shepherd, D. E. T. The barriers to the progression of additive manufacture: Perspectives from UK industry. *Int. J. Prod. Econ.* **198**, 104–118 (2018). 10.1016/J.IJPE.2018.02.003
 72. Bäuml, M. Welche nicht-klinischen Faktoren beeinflussen den Einsatz innovativer Implantate? Das Beispiel medikamentenfreisetzungsfähiger Koronarstents bei Patienten mit akutem Myokardinfarkt: Eine Mehrebenen-Regressionsanalyse. *Das Gesundheitswes.* **75**, 822–831 (2013). 10.1055/s-0033-1333739
 73. Cappellaro, G., Ghislandi, S. & Anessi-Pessina, E. Diffusion of medical technology: the role of financing. *Health Policy* **100**, 51–9 (2011). 10.1016/j.healthpol.2010.10.004
 74. Wilson, C. B. Adoption of new surgical technology. *BMJ* **332**, 112–4 (2006). 10.1136/bmj.332.7533.112
 75. Jardini, A. L. *et al.* Customised titanium implant fabricated in additive manufacturing for craniomaxillofacial surgery. *Virtual Phys. Prototyp.* **9**, 115–125 (2014). 10.1080/17452759.2014.900857

76. Bibb, R., Eggbeer, D., Evans, P., Bocca, A. & Sugar, A. Rapid manufacture of custom-fitting surgical guides. *Rapid Prototyp. J.* **15**, 346–354 (2009). 10.1108/13552540910993879
77. Tack, P., Victor, J., Gemmel, P. & Annemans, L. 3D-printing techniques in a medical setting: a systematic literature review. *Biomed. Eng. Online* **15**, 115 (2016). 10.1186/s12938-016-0236-4
78. Wen, C. E. *et al.* Processing and mechanical properties of autogenous titanium implant materials. *J. Mater. Sci. Mater. Med.* **13**, 397–401 (2002). 10.1023/A:1014344819558
79. Kováčik, J. Correlation between Young's modulus and porosity in porous materials. *J. Mater. Sci. Lett.* **18**, 1007–1010 (1999). 10.1023/A:1006669914946
80. Hulbert, S. F. *et al.* Potential of ceramic materials as permanently implantable skeletal prostheses. *J. Biomed. Mater. Res.* **4**, 433–456 (1970). 10.1002/jbm.820040309
81. Frosch, K.-H. *et al.* Growth behavior, matrix production, and gene expression of human osteoblasts in defined cylindrical titanium channels. *J. Biomed. Mater. Res. Part A* **68A**, 325–334 (2004). 10.1002/jbm.a.20010
82. Li, J. *et al.* Biological performance in goats of a porous titanium alloy–biphasic calcium phosphate composite. *Biomaterials* **28**, 4209–4218 (2007). 10.1016/J.BIOMATERIALS.2007.05.042
83. Turner, T. M., Sumner, D. R., Urban, R. M., Rivero, D. P. & Galante, J. O. A comparative study of porous coatings in a weight-bearing total hip-arthroplasty model. *J. Bone Joint Surg. Am.* **68**, 1396–409 (1986).
84. Van Bael, S. *et al.* The effect of pore geometry on the in vitro biological behavior of human periosteum-derived cells seeded on selective laser-melted Ti6Al4V bone scaffolds. *Acta Biomater.* **8**, 2824–2834 (2012). 10.1016/j.actbio.2012.04.001
85. Hollander, D. A. *et al.* Structural, mechanical and in vitro characterization of individually structured Ti–6Al–4V produced by direct laser forming. *Biomaterials* **27**, 955–963 (2006). 10.1016/J.BIOMATERIALS.2005.07.041
86. Warnke, P., Douglas, T., Wollny, P. & Sherry, E. Rapid Prototyping: Porous Titanium Alloy Scaffolds Produced by Selective Laser Melting for Bone Tissue Engineering. *Tissue Eng. Part C Methods* **15**, (2009).
87. Xue, W., Krishna, B. V., Bandyopadhyay, A. & Bose, S. Processing and biocompatibility evaluation of laser processed porous titanium. *Acta Biomater.* **3**, 1007–1018 (2007). 10.1016/J.ACTBIO.2007.05.009
88. Taniguchi, N. *et al.* Effect of pore size on bone ingrowth into porous titanium implants fabricated by additive manufacturing: An in vivo experiment. *Mater. Sci. Eng. C* **59**, 690–701 (2016). 10.1016/J.MSEC.2015.10.069
89. Balla, V. K., Bodhak, S., Bose, S. & Bandyopadhyay, A. Porous tantalum structures for bone implants: Fabrication, mechanical and in vitro biological properties. *Acta Biomater.* **6**, 3349–3359 (2010). 10.1016/J.ACTBIO.2010.01.046
90. Wu, S. H. *et al.* Porous Titanium-6 Aluminum-4 Vanadium Cage Has Better Osseointegration and Less Micromotion Than a Poly-Ether-Ether-Ketone Cage in Sheep Vertebral Fusion. *Artif. Organs* **37**, E191–E201 (2013). 10.1111/aor.12153
91. McGilvray, K. C. *et al.* Bony ingrowth potential of 3D-printed porous titanium alloy: a direct comparison of interbody cage materials in an in vivo ovine lumbar fusion model. *Spine J.* **18**, 1250–1260 (2018). 10.1016/j.spinee.2018.02.018
92. Plecko, M. *et al.* Osseointegration and biocompatibility of different metal implants--a comparative experimental investigation in sheep. *BMC Musculoskelet. Disord.* **13**, 32 (2012). 10.1186/1471-2474-13-32
93. Shah, F. A. *et al.* Long-term osseointegration of 3D printed CoCr constructs with an interconnected open-pore architecture prepared by electron beam melting. *Acta Biomater.* **36**, 296–309 (2016). 10.1016/J.ACTBIO.2016.03.033
94. Nune, K. C. *et al.* Functional response of osteoblasts in functionally gradient titanium alloy mesh arrays processed by 3D additive manufacturing. *Colloids Surfaces B Biointerfaces* **150**, 78–88 (2017). 10.1016/j.colsurfb.2016.09.050

95. Zhang, Z. *et al.* Hierarchical tailoring of strut architecture to control permeability of additive manufactured titanium implants. *Mater. Sci. Eng. C* **33**, 4055–4062 (2013). 10.1016/j.msec.2013.05.050
96. Bobyn, J. D. *et al.* Producing and avoiding stress shielding. Laboratory and clinical observations of noncemented total hip arthroplasty. *Clin. Orthop. Relat. Res.* 79–96 (1992).
97. Neugebauer, R. *et al.* Topology-Optimized Implants: Medical Requirements and Partial Aspects of a Design Engineering Process Chain. in *Future Trends in Production Engineering* 33–46 (Springer Berlin Heidelberg, 2013). doi:10.1007/978-3-642-24491-9_4 10.1007/978-3-642-24491-9_4
98. Fraldi, M. *et al.* Topological optimization in hip prosthesis design. *Biomech Model Mechanobiol* **9**, 389–402 (2010). 10.1007/s10237-009-0183-0
99. Oshkour, A. A., Osman, N. A. A., Bayat, M., Afshar, R. & Berto, F. Three-dimensional finite element analyses of functionally graded femoral prostheses with different geometrical configurations. *Mater. Des.* **56**, 998–1008 (2014). 10.1016/j.matdes.2013.12.054
100. Bandyopadhyay, A. & Heer, B. Additive manufacturing of multi-material structures. *Mater. Sci. Eng. R Reports* **129**, 1–16 (2018). 10.1016/J.MSER.2018.04.001
101. Sola, A., Bellucci, D. & Cannillo, V. Functionally graded materials for orthopedic applications – an update on design and manufacturing. *Biotechnol. Adv.* **34**, 504–531 (2016). 10.1016/j.biotechadv.2015.12.013
102. Panesar, A., Abdi, M., Hickman, D. & Ashcroft, I. Strategies for functionally graded lattice structures derived using topology optimisation for Additive Manufacturing. *Addit. Manuf.* **19**, 81–94 (2018). 10.1016/J.ADDMA.2017.11.008
103. Wang, X. *et al.* Topological design and additive manufacturing of porous metals for bone scaffolds and orthopaedic implants: A review. *Biomaterials* **83**, 127–141 (2016). 10.1016/j.biomaterials.2016.01.012
104. Harrysson, O. L. A., Cansizoglu, O., Marcellin-Little, D. J., Cormier, D. R. & West, H. A. Direct metal fabrication of titanium implants with tailored materials and mechanical properties using electron beam melting technology. *Mater. Sci. Eng. C* **28**, 366–373 (2008). 10.1016/J.MSEC.2007.04.022
105. Arabnejad, S., Johnston, B., Tanzer, M. & Pasini, D. Fully porous 3D printed titanium femoral stem to reduce stress-shielding following total hip arthroplasty. *J. Orthop. Res.* **35**, 1774–1783 (2017). 10.1002/jor.23445
106. Rahimizadeh, A., Nourmohammadi, Z., Arabnejad, S., Tanzer, M. & Pasini, D. Porous architected biomaterial for a tibial-knee implant with minimum bone resorption and bone-implant interface micromotion. *J. Mech. Behav. Biomed. Mater.* **78**, 465–479 (2018). 10.1016/J.JMBBM.2017.11.041
107. Fousová, M., Vojtěch, D., Kubásek, J., Jablonská, E. & Fojt, J. Promising characteristics of gradient porosity Ti-6Al-4V alloy prepared by SLM process. *J. Mech. Behav. Biomed. Mater.* **69**, 368–376 (2017). 10.1016/j.jmbbm.2017.01.043
108. Hazlehurst, K. B., Wang, C. J. & Stanford, M. An investigation into the flexural characteristics of functionally graded cobalt chrome femoral stems manufactured using selective laser melting. *Mater. Des.* **60**, 177–183 (2014). 10.1016/J.MATDES.2014.03.068
109. Limmahakhun, S., Oloyede, A., Sithiseripratip, K., Xiao, Y. & Yan, C. Stiffness and strength tailoring of cobalt chromium graded cellular structures for stress-shielding reduction. *Mater. Des.* **114**, 633–641 (2017). 10.1016/J.MATDES.2016.11.090
110. Simoneau, C., Terriault, P., Jetté, B., Dumas, M. & Brailovski, V. Development of a porous metallic femoral stem: Design, manufacturing, simulation and mechanical testing. *Mater. Des.* **114**, 546–556 (2017). 10.1016/J.MATDES.2016.10.064
111. Zhao, S. *et al.* Compressive and fatigue behavior of functionally graded Ti-6Al-4V meshes fabricated by electron beam melting. *Acta Mater.* **150**, 1–15 (2018). 10.1016/J.ACTAMAT.2018.02.060
112. Ning, C. *et al.* Concentration Ranges of Antibacterial Cations for Showing the Highest

- Antibacterial Efficacy but the Least Cytotoxicity against Mammalian Cells: Implications for a New Antibacterial Mechanism. *Chem. Res. Toxicol.* **28**, 1815–1822 (2015). 10.1021/acs.chemrestox.5b00258
113. Maskery, I. *et al.* An investigation into reinforced and functionally graded lattice structures. *J. Cell. Plast.* **53**, 151–165 (2017). 10.1177/0021955X16639035
 114. Xiao, L. & Song, W. Additively-manufactured functionally graded Ti-6Al-4V lattice structures with high strength under static and dynamic loading: Experiments. *Int. J. Impact Eng.* **111**, 255–272 (2018). 10.1016/J.IJIMPENG.2017.09.018
 115. Zhang, X.-Y., Fang, G., Xing, L.-L., Liu, W. & Zhou, J. Effect of porosity variation strategy on the performance of functionally graded Ti-6Al-4V scaffolds for bone tissue engineering. *Mater. Des.* **157**, 523–538 (2018). 10.1016/J.MATDES.2018.07.064
 116. Aremu, A. O. *et al.* A voxel-based method of constructing and skinning conformal and functionally graded lattice structures suitable for additive manufacturing. *Addit. Manuf.* **13**, 1–13 (2017). 10.1016/J.ADDMA.2016.10.006
 117. Brennan-Craddock, J., Brackett, D., Wildman, R. & Hague, R. The design of impact absorbing structures for additive manufacture. *J. Phys. Conf. Ser.* **382**, 012042 (2012). 10.1088/1742-6596/382/1/012042
 118. Alt, V. Antimicrobial coated implants in trauma and orthopaedics—A clinical review and risk-benefit analysis. *Injury* **48**, 599–607 (2017). 10.1016/j.injury.2016.12.011
 119. Froimson, M. I., Garino, J., Machenau, A. & Vidalain, J. P. Minimum 10-year results of a tapered, titanium, hydroxyapatite-coated hip stem: an independent review. *J. Arthroplasty* **22**, 1–7 (2007). 10.1016/j.arth.2006.03.003
 120. Epinette, J.-A. Long lasting outcome of hydroxyapatite-coated implants in primary knee arthroplasty: a continuous series of two hundred and seventy total knee arthroplasties at fifteen to twenty two years of clinical follow-up. *Int. Orthop.* **38**, 305–311 (2014). 10.1007/s00264-013-2246-1
 121. Giannitelli, S. M., Mozetic, P., Trombetta, M. & Rainer, A. Combined additive manufacturing approaches in tissue engineering. *Acta Biomater.* **24**, 1–11 (2015). 10.1016/J.ACTBIO.2015.06.032
 122. Mager, V. RESEARCH ON INFILTRATING BIOCOMPATIBLE FILLERS TO PRODUCE COMPOSITE IMPLANTS. *Acad. J. Manuf. Eng.* **11**, (2013).
 123. Liu, H. *et al.* Incorporating simvastatin/poloxamer 407 hydrogel into 3D-printed porous Ti₆Al₄V scaffolds for the promotion of angiogenesis, osseointegration and bone ingrowth. *Biofabrication* **8**, 045012 (2016). 10.1088/1758-5090/8/4/045012
 124. Cox, S. C. *et al.* Adding functionality with additive manufacturing: Fabrication of titanium-based antibiotic eluting implants. *Mater. Sci. Eng. C* **64**, 407–415 (2016). 10.1016/j.msec.2016.04.006
 125. Hassanin, H. *et al.* Tailoring selective laser melting process for titanium drug-delivering implants with releasing micro-channels. *Addit. Manuf.* **20**, 144–155 (2018). 10.1016/J.ADDMA.2018.01.005
 126. Bezuidenhout, M. B., van Staden, A. D., Oosthuizen, G. A., Dimitrov, D. M. & Dicks, L. M. T. Delivery of Antibiotics from Cementless Titanium-Alloy Cubes May Be a Novel Way to Control Postoperative Infections. *Biomed Res. Int.* **2015**, 1–7 (2015). 10.1155/2015/856859
 127. Bobrowski, T. & Schuhmann, W. Long-term implantable glucose biosensors. *Curr. Opin. Electrochem.* **10**, 112–119 (2018). 10.1016/J.COEELEC.2018.05.004
 128. Shasha Liu, P. & Tse, H.-F. Implantable sensors for heart failure monitoring. *J. Arrhythmia* **29**, 314–319 (2013). 10.1016/J.JOA.2013.06.003
 129. Frost, M. C. & Meyerhoff, M. E. Implantable chemical sensors for real-time clinical monitoring: progress and challenges. *Curr. Opin. Chem. Biol.* **6**, 633–641 (2002). 10.1016/S1367-5931(02)00371-X
 130. Vaddiraju, S., Tomazos, I., Burgess, D. J., Jain, F. C. & Papadimitrakopoulos, F. Emerging synergy between nanotechnology and implantable biosensors: A review. *Biosens. Bioelectron.* **25**, 1553–1565 (2010). 10.1016/J.BIOS.2009.12.001
 131. Bergmann, G., Bender, A., Dymke, J., Duda, G. & Damm, P. Standardized Loads

- Acting in Hip Implants. *PLoS One* **11**, e0155612 (2016).
10.1371/journal.pone.0155612
132. Bottner, F. *et al.* Interleukin-6, procalcitonin and TNF- α . *J. Bone Joint Surg. Br.* **89-B**, 94–99 (2007). 10.1302/0301-620X.89B1.17485
 133. Niinomi, M., Nakai, M. & Hieda, J. Development of new metallic alloys for biomedical applications. *Acta Biomater.* **8**, 3888–3903 (2012). 10.1016/J.ACTBIO.2012.06.037
 134. Elahinia, M. *et al.* Fabrication of NiTi through additive manufacturing: A review. *Prog. Mater. Sci.* **83**, 630–663 (2016). 10.1016/J.PMATSCI.2016.08.001
 135. Yadroitsev, I., Krakhmalev, P. & Yadroitsava, I. Titanium Alloys Manufactured by In Situ Alloying During Laser Powder Bed Fusion. *JOM* **69**, 2725–2730 (2017). 10.1007/s11837-017-2600-7
 136. Didier, P., Piotrowski, B., Fischer, M. & Laheurte, P. Mechanical stability of custom-made implants: Numerical study of anatomical device and low elastic Young's modulus alloy. *Mater. Sci. Eng. C* **74**, 399–409 (2017). 10.1016/j.msec.2016.12.031
 137. Liu, J., Ruan, J., Chang, L., Yang, H. & Ruan, W. Porous Nb-Ti-Ta alloy scaffolds for bone tissue engineering: Fabrication, mechanical properties and in vitro/vivo biocompatibility. *Mater. Sci. Eng. C* **78**, 503–512 (2017). 10.1016/J.MSEC.2017.04.088
 138. Liu, Y. J., Li, X. P., Zhang, L. C. & Sercombe, T. B. Processing and properties of topologically optimised biomedical Ti–24Nb–4Zr–8Sn scaffolds manufactured by selective laser melting. *Mater. Sci. Eng. A* **642**, 268–278 (2015). 10.1016/j.msea.2015.06.088
 139. Szymczyk, P. *et al.* The ability of *S.aureus* to form biofilm on the Ti-6Al-7Nb scaffolds produced by Selective Laser Melting and subjected to the different types of surface modifications. *Acta Bioeng. Biomech.* **15**, 69–76 (2013). 10.5277/abb130109
 140. Speirs, M., Humbeeck, J. V., Schrooten, J., Luyten, J. & Kruth, J. P. The Effect of Pore Geometry on the Mechanical Properties of Selective Laser Melted Ti-13Nb-13Zr Scaffolds. *Procedia CIRP* **5**, 79–82 (2013). 10.1016/j.procir.2013.01.016
 141. Wang, Q. *et al.* Effect of Nb content on microstructure, property and in vitro apatite-forming capability of Ti-Nb alloys fabricated via selective laser melting. *Mater. Des.* **126**, 268–277 (2017). 10.1016/j.matdes.2017.04.026
 142. Yan, L. *et al.* Improved mechanical properties of the new Ti-15Ta-xZr alloys fabricated by selective laser melting for biomedical application. *J. Alloys Compd.* **688**, 156–162 (2016). 10.1016/J.JALLCOM.2016.07.002
 143. Vrancken, B., Thijs, L., Kruth, J.-P. & Van Humbeeck, J. Heat treatment of Ti6Al4V produced by Selective Laser Melting: Microstructure and mechanical properties. *J. Alloys Compd.* **541**, 177–185 (2012). 10.1016/J.JALLCOM.2012.07.022
 144. Barbas, A., Bonnet, A.-S., Lipinski, P., Pesci, R. & Dubois, G. Development and mechanical characterization of porous titanium bone substitutes. *J. Mech. Behav. Biomed. Mater.* **9**, 34–44 (2012). 10.1016/J.JMBBM.2012.01.008
 145. Schulze, C., Weinmann, M., Schweigel, C., Keßler, O. & Bader, R. Mechanical Properties of a Newly Additive Manufactured Implant Material Based on Ti-42Nb. *Materials (Basel)*. **11**, 124 (2018). 10.3390/ma11010124
 146. Sing, S. L., Yeong, W. Y. & Wiria, F. E. Selective laser melting of titanium alloy with 50 wt% tantalum: Microstructure and mechanical properties. *J. Alloys Compd.* **660**, 461–470 (2016). 10.1016/J.JALLCOM.2015.11.141
 147. Vrancken, B., Thijs, L., Kruth, J.-P. & Van Humbeeck, J. Microstructure and mechanical properties of a novel β titanium metallic composite by selective laser melting. *Acta Mater.* **68**, 150–158 (2014). 10.1016/j.actamat.2014.01.018
 148. Ouyang, D., Li, N., Xing, W., Zhang, J. & Liu, L. 3D printing of crack-free high strength Zr-based bulk metallic glass composite by selective laser melting. *Intermetallics* **90**, 128–134 (2017). 10.1016/J.INTERMET.2017.07.010
 149. Pauly, S., Schricker, C., Scudino, S., Deng, L. & Kühn, U. Processing a glass-forming Zr-based alloy by selective laser melting. *Mater. Des.* **135**, 133–141 (2017). 10.1016/J.MATDES.2017.08.070

150. Hoffmeister, B. K., Smith, S. R., Handley, S. M. & Rho, J. Y. Anisotropy of Young's modulus of human tibial cortical bone. *Med. Biol. Eng. Comput.* **38**, 333–8 (2000).
151. Deng, L., Wang, S., Wang, P., Kühn, U. & Pauly, S. Selective laser melting of a Ti-based bulk metallic glass. *Mater. Lett.* **212**, 346–349 (2018). 10.1016/J.MATLET.2017.10.130
152. Cordeiro, J. M. & Barão, V. A. R. Is there scientific evidence favoring the substitution of commercially pure titanium with titanium alloys for the manufacture of dental implants? *Mater. Sci. Eng. C* **71**, 1201–1215 (2017). 10.1016/j.msec.2016.10.025
153. U.S. Food & Drug Administration. Class 2 Device Recall Accolade TMZF Plus Hip Stem. (2011). Available at: <https://www.accessdata.fda.gov/scripts/cdrh/cfdocs/cfres/res.cfm?id=99392#2>. (Accessed: 4th October 2018)
154. Yang, X. & Hutchinson, C. R. Corrosion-wear of β -Ti alloy TMZF (Ti-12Mo-6Zr-2Fe) in simulated body fluid. *Acta Biomater.* **42**, 429–439 (2016). 10.1016/J.ACTBIO.2016.07.008
155. Khoo, Z. X. *et al.* A Review of Selective Laser Melted NiTi Shape Memory Alloy. *Mater. (Basel, Switzerland)* **11**, (2018). 10.3390/ma11040519
156. Li, H. F. & Zheng, Y. F. Recent advances in bulk metallic glasses for biomedical applications. *Acta Biomater.* **6**, 2740–2750 (2016). 10.1016/j.actbio.2016.03.047
157. Jung, H. Y. *et al.* Fabrication of Fe-based bulk metallic glass by selective laser melting: A parameter study. *Mater. Des.* **86**, 703–708 (2015). 10.1016/J.MATDES.2015.07.145
158. Zhang, Y. *et al.* Amorphous alloy strengthened stainless steel manufactured by selective laser melting: Enhanced strength and improved corrosion resistance. *Scr. Mater.* **148**, 20–23 (2018). 10.1016/J.SCRIPTAMAT.2018.01.016
159. Pauly, S. *et al.* Processing metallic glasses by selective laser melting. *Mater. Today* **16**, 37–41 (2013). 10.1016/J.MATTOD.2013.01.018
160. Lin, X. *et al.* Orthopedic implant biomaterials with both osteogenic and anti-infection capacities and associated in vivo evaluation methods. *Nanomedicine Nanotechnology, Biol. Med.* **13**, 123–142 (2017). 10.1016/j.nano.2016.08.003
161. Wei, Q. *et al.* Selective laser melting of stainless-steel/nano-hydroxyapatite composites for medical applications: Microstructure, element distribution, crack and mechanical properties. *J. Mater. Process. Technol.* **222**, 444–453 (2015). 10.1016/J.JMATPROTEC.2015.02.010
162. Hao, L., Dadbakhsh, S., Seaman, O. & Felstead, M. Selective laser melting of a stainless steel and hydroxyapatite composite for load-bearing implant development. *J. Mater. Process. Technol.* **209**, 5793–5801 (2009). 10.1016/J.JMATPROTEC.2009.06.012
163. Han, C. *et al.* Microstructure and property evolutions of titanium/nano-hydroxyapatite composites in-situ prepared by selective laser melting. *J. Mech. Behav. Biomed. Mater.* **71**, 85–94 (2017). 10.1016/J.JMBBM.2017.02.021
164. Han, C. *et al.* Titanium/hydroxyapatite (Ti/HA) gradient materials with quasi-continuous ratios fabricated by SLM: Material interface and fracture toughness. *Mater. Des.* **141**, 256–266 (2018). 10.1016/J.MATDES.2017.12.037
165. Marcu, T., Menapace, C., Girardini, L., Leordean, D. & Popa, C. Selective laser melting of Ti6Al7Nb with hydroxyapatite addition. *Rapid Prototyp. J.* **20**, 301–310 (2014).
166. Shishkovskii, I. V., Yadroitsev, I. A. & Smurov, I. Y. Selective laser sintering/melting of nitinol–hydroxyapatite composite for medical applications. *Powder Metall. Met. Ceram.* **50**, 275–283 (2011). 10.1007/s11106-011-9329-6
167. Shuai, C. *et al.* Biodegradation Resistance and Bioactivity of Hydroxyapatite Enhanced Mg-Zn Composites via Selective Laser Melting. *Materials (Basel)*. **10**, 307 (2017). 10.3390/ma10030307
168. Wang, Q. *et al.* Antimicrobial Cu-bearing stainless steel scaffolds. *Mater. Sci. Eng. C* **68**, 519–522 (2016). 10.1016/J.MSEC.2016.06.038

169. Xi, T. *et al.* Effect of copper addition on mechanical properties, corrosion resistance and antibacterial property of 316L stainless steel. *Mater. Sci. Eng. C* **71**, 1079–1085 (2017). 10.1016/J.MSEC.2016.11.022
170. Krakhmalev, P., Yadroitsev, I., Yadroitsava, I. & de Smidt, O. Functionalization of Biomedical Ti6Al4V via In Situ Alloying by Cu during Laser Powder Bed Fusion Manufacturing. *Materials (Basel)*. **10**, 1154 (2017). 10.3390/ma10101154
171. Macpherson, A. *et al.* Antibacterial Titanium Produced Using Selective Laser Melting. *JOM* 1–6 (2017). doi:10.1007/s11837-017-2589-y 10.1007/s11837-017-2589-y
172. Guo, S. *et al.* Preliminary study on the corrosion resistance, antibacterial activity and cytotoxicity of selective-laser-melted Ti6Al4V-xCu alloys. *Mater. Sci. Eng. C* **72**, 631–640 (2017). 10.1016/J.MSEC.2016.11.126
173. Luo, J. *et al.* Cytocompatibility of Cu-bearing Ti6Al4V alloys manufactured by selective laser melting. *Mater. Charact.* (2017). doi:10.1016/J.MATCHAR.2017.12.003 10.1016/J.MATCHAR.2017.12.003
174. Lu, Y. *et al.* CoCrWCu alloy with antibacterial activity fabricated by selective laser melting: Densification, mechanical properties and microstructural analysis. *Powder Technol.* **325**, 289–300 (2018). 10.1016/J.POWTEC.2017.11.018
175. Luo, J. *et al.* The effect of 3 wt.% Cu addition on the microstructure, tribological property and corrosion resistance of CoCrW alloys fabricated by selective laser melting. *J. Mater. Sci. Mater. Med.* **29**, 37 (2018). 10.1007/s10856-018-6043-7
176. Ren, L. *et al.* A novel coping metal material CoCrCu alloy fabricated by selective laser melting with antimicrobial and antibiofilm properties. *Mater. Sci. Eng. C* **67**, 461–467 (2016). 10.1016/J.MSEC.2016.05.069
177. Shuai, C. *et al.* Microstructure, biodegradation, antibacterial and mechanical properties of ZK60-Cu alloys prepared by selective laser melting technique. *J. Mater. Sci. Technol.* **34**, 1944–1952 (2018). 10.1016/J.JMST.2018.02.006
178. Shuai, C. *et al.* Ag-Introduced Antibacterial Ability and Corrosion Resistance for Bio-Mg Alloys. *Biomed Res. Int.* **2018**, 1–13 (2018). 10.1155/2018/6023460
179. Chen, M. *et al.* Effect of nano/micro-Ag compound particles on the bio-corrosion, antibacterial properties and cell biocompatibility of Ti-Ag alloys. *Mater. Sci. Eng. C* **75**, 906–917 (2017). 10.1016/j.msec.2017.02.142
180. Stenlund, P. *et al.* Osseointegration Enhancement by Zr doping of Co-Cr-Mo Implants Fabricated by Electron Beam Melting. *Addit. Manuf.* **6**, 6–15 (2015). 10.1016/J.ADDMA.2015.02.002
181. Shah, F. A., Jergéus, E., Chiba, A. & Palmquist, A. Osseointegration of 3D printed microalloyed CoCr implants-Addition of 0.04% Zr to CoCr does not alter bone material properties. *J. Biomed. Mater. Res. Part A* **106**, 1655–1663 (2018). 10.1002/jbm.a.36366
182. Haude, M. *et al.* Safety and performance of the drug-eluting absorbable metal scaffold (DREAMS) in patients with de-novo coronary lesions: 12 month results of the prospective, multicentre, first-in-man BIOSOLVE-I trial. *Lancet* **381**, 836–844 (2013). 10.1016/S0140-6736(12)61765-6
183. Windhagen, H. *et al.* Biodegradable magnesium-based screw clinically equivalent to titanium screw in hallux valgus surgery: short term results of the first prospective, randomized, controlled clinical pilot study. *Biomed. Eng. Online* **12**, 62 (2013). 10.1186/1475-925X-12-62
184. Lee, J.-W. *et al.* Long-term clinical study and multiscale analysis of in vivo biodegradation mechanism of Mg alloy. *Proc. Natl. Acad. Sci. U. S. A.* **113**, 716–21 (2016). 10.1073/pnas.1518238113
185. Zhao, D. *et al.* Vascularized bone grafting fixed by biodegradable magnesium screw for treating osteonecrosis of the femoral head. *Biomaterials* **81**, 84–92 (2016). 10.1016/J.BIOMATERIALS.2015.11.038
186. Witte, F. Reprint of: The history of biodegradable magnesium implants: A review. *Acta Biomaterialia* **23**, S28–S40 (2015). 10.1016/j.actbio.2015.07.017
187. Zheng, Y. F., Gu, X. N. & Witte, F. Biodegradable metals. *Mater. Sci. Eng. R Reports*

- 77, 1–34 (2014). 10.1016/J.MSER.2014.01.001
188. Yusop, A. H., Bakir, A. A., Shaharom, N. A., Abdul Kadir, M. R. & Hermawan, H. Porous Biodegradable Metals for Hard Tissue Scaffolds: A Review. *Int. J. Biomater.* **2012**, 1–10 (2012). 10.1155/2012/641430
 189. Roland, L. *et al.* Poly- ϵ -caprolactone Coated and Functionalized Porous Titanium and Magnesium Implants for Enhancing Angiogenesis in Critically Sized Bone Defects. *Int. J. Mol. Sci.* **17**, 1 (2015). 10.3390/ijms17010001
 190. Li, Y. *et al.* Additively manufactured biodegradable porous magnesium. *Acta Biomater.* (2017). doi:10.1016/J.ACTBIO.2017.12.008 10.1016/J.ACTBIO.2017.12.008
 191. Grau, M. *et al.* Osteointegration of Porous Poly- ϵ -Caprolactone-Coated and Previtallised Magnesium Implants in Critically Sized Calvarial Bone Defects in the Mouse Model. *Materials (Basel)*. **11**, 6 (2017). 10.3390/ma11010006
 192. Chen, Y., Xu, Z., Smith, C. & Sankar, J. Recent advances on the development of magnesium alloys for biodegradable implants. *Acta Biomater.* **10**, 4561–4573 (2014). 10.1016/J.ACTBIO.2014.07.005
 193. Ibrahim, H., Esfahani, S. N., Poorganji, B., Dean, D. & Elahinia, M. Resorbable bone fixation alloys, forming, and post-fabrication treatments. *Mater. Sci. Eng. C* **70**, 870–888 (2017). 10.1016/J.MSEC.2016.09.069
 194. Hu, D. *et al.* Experimental Investigation on Selective Laser Melting of Bulk Net-Shape Pure Magnesium. *Mater. Manuf. Process.* **30**, 1298–1304 (2015). 10.1080/10426914.2015.1025963
 195. Matena, J. *et al.* Comparison of Selective Laser Melted Titanium and Magnesium Implants Coated with PCL. *Int. J. Mol. Sci.* **16**, 13287–13301 (2015). 10.3390/ijms160613287
 196. Wei, K., Gao, M., Wang, Z. & Zeng, X. Effect of energy input on formability, microstructure and mechanical properties of selective laser melted AZ91D magnesium alloy. *Mater. Sci. Eng. A* **611**, 212–222 (2014). 10.1016/J.MSEA.2014.05.092
 197. Schmid, D., Renza, J., Zaeh, M. F. & Glasschroeder, J. Process Influences on Laser-beam Melting of the Magnesium Alloy AZ91. *Phys. Procedia* **83**, 927–936 (2016). 10.1016/J.PHPRO.2016.08.097
 198. Long, T. *et al.* Novel Mg-based alloys by selective laser melting for biomedical applications: microstructure evolution, microhardness and *in vitro* degradation behaviour. *Virtual Phys. Prototyp.* 1–11 (2017). doi:10.1080/17452759.2017.1411662 10.1080/17452759.2017.1411662
 199. He, C. *et al.* Microstructure Evolution and Biodegradation Behavior of Laser Rapid Solidified Mg–Al–Zn Alloy. *Metals (Basel)*. **7**, 105 (2017). 10.3390/met7030105
 200. Liu, C., Zhang, M. & Chen, C. Effect of laser processing parameters on porosity, microstructure and mechanical properties of porous Mg–Ca alloys produced by laser additive manufacturing. *Mater. Sci. Eng. A* **703**, 359–371 (2017). 10.1016/J.MSEA.2017.07.031
 201. Denkena, B. & Lucas, A. Biocompatible Magnesium Alloys as Absorbable Implant Materials – Adjusted Surface and Subsurface Properties by Machining Processes. *CIRP Ann.* **56**, 113–116 (2007). 10.1016/J.CIRP.2007.05.029
 202. Wei, K., Wang, Z. & Zeng, X. Influence of element vaporization on formability, composition, microstructure, and mechanical performance of the selective laser melted Mg–Zn–Zr components. *Mater. Lett.* **156**, 187–190 (2015). 10.1016/J.MATLET.2015.05.074
 203. Grasso, M., Demir, A. G., Previtali, B. & Colosimo, B. M. In situ monitoring of selective laser melting of zinc powder via infrared imaging of the process plume. *Robot. Comput. Integr. Manuf.* **49**, 229–239 (2018). 10.1016/J.RCIM.2017.07.001
 204. Montani, M., Demir, A. G., Mostaed, E., Vedani, M. & Previtali, B. Processability of pure Zn and pure Fe by SLM for biodegradable metallic implant manufacturing. *Rapid Prototyp. J.* **23**, 514–523 (2017). 10.1108/RPJ-08-2015-0100

205. Demir, A. G., Monguzzi, L. & Previtali, B. Selective laser melting of pure Zn with high density for biodegradable implant manufacturing. *Addit. Manuf.* **15**, 20–28 (2017). 10.1016/J.ADDMA.2017.03.004
206. Wen, P. *et al.* Densification behavior of pure Zn metal parts produced by selective laser melting for manufacturing biodegradable implants. *J. Mater. Process. Technol.* **258**, 128–137 (2018). 10.1016/J.JMATPROTEC.2018.03.007
207. Niendorf, T. *et al.* Processing of New Materials by Additive Manufacturing: Iron-Based Alloys Containing Silver for Biomedical Applications. *Metall. Mater. Trans. A* **46**, 2829–2833 (2015). 10.1007/s11661-015-2932-2
208. Rim, K. T., Koo, K. H. & Park, J. S. Toxicological Evaluations of Rare Earths and Their Health Impacts to Workers: A Literature Review. *Saf. Health Work* **4**, 12–26 (2013). 10.5491/SHAW.2013.4.1.12
209. Frazier, W. E. Metal Additive Manufacturing: A Review. *J. Mater. Eng. Perform.* **23**, 1917–1928 (2014). 10.1007/s11665-014-0958-z
210. Mower, T. M. & Long, M. J. Mechanical behavior of additive manufactured, powder-bed laser-fused materials. *Mater. Sci. Eng. A* **651**, 198–213 (2016). 10.1016/J.MSEA.2015.10.068
211. Haan, J. *et al.* Effect of subsequent Hot Isostatic Pressing on mechanical properties of ASTM F75 alloy produced by Selective Laser Melting. *Powder Metall.* **58**, 161–165 (2015). 10.1179/0032589915Z.000000000236
212. Leuders, S. *et al.* On the mechanical behaviour of titanium alloy TiAl6V4 manufactured by selective laser melting: Fatigue resistance and crack growth performance. *Int. J. Fatigue* **48**, 300–307 (2013). 10.1016/J.IJFATIGUE.2012.11.011
213. Molaei, R., Fatemi, A. & Phan, N. Significance of hot isostatic pressing (HIP) on multiaxial deformation and fatigue behaviors of additive manufactured Ti-6Al-4V including build orientation and surface roughness effects. *Int. J. Fatigue* **117**, 352–370 (2018). 10.1016/J.IJFATIGUE.2018.07.035
214. Everton, S. K., Hirsch, M., Stravoulakis, P., Leach, R. K. & Clare, A. T. Review of in-situ process monitoring and in-situ metrology for metal additive manufacturing. *Mater. Des.* **95**, 431–445 (2016). 10.1016/J.MATDES.2016.01.099
215. Arcam AB. Process Validation Tools - Arcam AB. Available at: <http://www.arcam.com/technology/electron-beam-melting/process-validation-tools/>. (Accessed: 4th October 2018)
216. ConceptLaser. ConceptLaser Products: Quality Management. Available at: <https://www.concept-laser.de/en/products/quality-management.html>. (Accessed: 4th October 2018)
217. EOS. Monitoring of industrial 3D printing processes. Available at: <https://www.eos.info/software/monitoring-software>. (Accessed: 4th October 2018)
218. Renishaw PLC. Renishaw InfiniAM Spectral. (2018). Available at: <http://www.renishaw.com/en/infiniam-spectral--42310>. (Accessed: 4th October 2018)
219. Hou, S. *et al.* Optimising the Dynamic Process Parameters in Electron Beam Melting (EBM) to Achieve Internal Defect Quality Control. *Proc. Int. Euro Powder Metall. Congr. Exhib. Euro PM 2017* (2017).
220. Kasperovich, G., Haubrich, J., Gussone, J. & Requena, G. Correlation between porosity and processing parameters in TiAl6V4 produced by selective laser melting. *Mater. Des.* **105**, 160–170 (2016). 10.1016/J.MATDES.2016.05.070
221. Rabin, B. H., Smolik, G. R. & Korth, G. E. Characterization of entrapped gases in rapidly solidified powders. *Mater. Sci. Eng. A* **124**, 1–7 (1990). 10.1016/0921-5093(90)90328-Z
222. Medina, F. Reducing metal alloy powder costs for use in powder bed fusion additive manufacturing: Improving the economics for production. *ETD Collect. Univ. Texas, El Paso* (2013).
223. Tamas-Williams, S. *et al.* XCT analysis of the influence of melt strategies on defect population in Ti-6Al-4V components manufactured by Selective Electron Beam Melting. *Mater. Charact.* **102**, 47–61 (2015). 10.1016/J.MATCHAR.2015.02.008

224. Zhang, W. *et al.* Effect of powder oxygen content on the microstructure and properties of Co–Cr dental alloys fabricated by selective laser melting. *Powder Metall.* **61**, 157–163 (2018). 10.1080/00325899.2017.1423200
225. Galarraga, H., Lados, D. A., Dehoff, R. R., Kirka, M. M. & Nandwana, P. Effects of the microstructure and porosity on properties of Ti-6Al-4V ELI alloy fabricated by electron beam melting (EBM). *Addit. Manuf.* **10**, 47–57 (2016). 10.1016/j.addma.2016.02.003
226. Gong, H., Rafi, K., Gu, H., Starr, T. & Stucker, B. Analysis of defect generation in Ti–6Al–4V parts made using powder bed fusion additive manufacturing processes. *Addit. Manuf.* **1–4**, 87–98 (2014). 10.1016/J.ADDMA.2014.08.002
227. Thijs, L., Verhaeghe, F., Craeghs, T., Humbeeck, J. Van & Kruth, J.-P. A study of the microstructural evolution during selective laser melting of Ti–6Al–4V. *Acta Mater.* **58**, 3303–3312 (2010). 10.1016/J.ACTAMAT.2010.02.004
228. Vilaro, T., Colin, C. & Bartout, J. D. As-Fabricated and Heat-Treated Microstructures of the Ti-6Al-4V Alloy Processed by Selective Laser Melting. *Metall. Mater. Trans. A* **42**, 3190–3199 (2011). 10.1007/s11661-011-0731-y
229. Edwards, P. & Ramulu, M. Fatigue performance evaluation of selective laser melted Ti–6Al–4V. *Mater. Sci. Eng. A* **598**, 327–337 (2014). 10.1016/J.MSEA.2014.01.041
230. Kok, Y. *et al.* Anisotropy and heterogeneity of microstructure and mechanical properties in metal additive manufacturing: A critical review. *Mater. Des.* **139**, 565–586 (2018). 10.1016/J.MATDES.2017.11.021
231. Darvish, K., Chen, Z. W., Phan, M. A. L. & Pasang, T. Selective laser melting of Co-29Cr-6Mo alloy with laser power 180–360 W: Cellular growth, intercellular spacing and the related thermal condition. *Mater. Charact.* **135**, 183–191 (2018). 10.1016/J.MATCHAR.2017.11.042
232. Zhou, X. *et al.* Textures formed in a CoCrMo alloy by selective laser melting. *J. Alloys Compd.* **631**, 153–164 (2015). 10.1016/J.JALLCOM.2015.01.096
233. Tan, X. P. *et al.* Carbide precipitation characteristics in additive manufacturing of Co-Cr-Mo alloy via selective electron beam melting. *Scr. Mater.* **143**, 117–121 (2018). 10.1016/J.SCRIPTAMAT.2017.09.022
234. Xu, W., Lui, E. W., Pateras, A., Qian, M. & Brandt, M. In situ tailoring microstructure in additively manufactured Ti-6Al-4V for superior mechanical performance. *Acta Mater.* **125**, 390–400 (2017). 10.1016/j.actamat.2016.12.027
235. Kang, N. *et al.* On the texture, phase and tensile properties of commercially pure Ti produced via selective laser melting assisted by static magnetic field. *Mater. Sci. Eng. C* **70**, 405–407 (2017). 10.1016/J.MSEC.2016.09.011
236. Peng, L., Bai, J., Zeng, X. & Zhou, Y. Comparison of isotropic and orthotropic material property assignments on femoral finite element models under two loading conditions. *Med. Eng. Phys.* **28**, 227–33 (2006). 10.1016/j.medengphy.2005.06.003
237. Nakano, T., Ishimoto, T. & Hagihara, K. Control of Morphological and Microstructural Anisotropy through Powder-Based Metal Additive Manufacturing. *J. Jpn. Soc. Powder Powder Metall.* **64**,
238. Popovich, V. A. *et al.* Functionally graded Inconel 718 processed by additive manufacturing: Crystallographic texture, anisotropy of microstructure and mechanical properties. *Mater. Des.* **114**, 441–449 (2017). 10.1016/j.matdes.2016.10.075
239. Ishimoto, T., Hagihara, K., Hisamoto, K., Sun, S.-H. & Nakano, T. Crystallographic texture control of beta-type Ti–15Mo–5Zr–3Al alloy by selective laser melting for the development of novel implants with a biocompatible low Young's modulus. *Scr. Mater.* **132**, 34–38 (2017). 10.1016/J.SCRIPTAMAT.2016.12.038
240. Wang, X. *et al.* Selective laser melting produced layer-structured NiTi shape memory alloys with high damping properties and Elinvar effect. *Scr. Mater.* **146**, 246–250 (2018). 10.1016/J.SCRIPTAMAT.2017.11.047
241. Chambrone, L., Shibli, J. A., Mercúrio, C. E., Cardoso, B. & Preshaw, P. M. Efficacy of standard (SLA) and modified sandblasted and acid-etched (SLActive) dental implants in promoting immediate and/or early occlusal loading protocols: a systematic review of prospective studies. *Clin. Oral Implants Res.* **26**, 359–370 (2015). 10.1111/clr.12347

242. Gittens, R. A. *et al.* The effects of combined micron-/submicron-scale surface roughness and nanoscale features on cell proliferation and differentiation. *Biomaterials* **32**, 3395–3403 (2011). 10.1016/J.BIOMATERIALS.2011.01.029
243. Oka, Y. I., Ohnogi, H., Hosokawa, T. & Matsumura, M. The impact angle dependence of erosion damage caused by solid particle impact. *Wear* **203–204**, 573–579 (1997). 10.1016/S0043-1648(96)07430-3
244. Cox, S. C. *et al.* Surface Finish has a Critical Influence on Biofilm Formation and Mammalian Cell Attachment to Additively Manufactured Prosthetics. *ACS Biomater. Sci. Eng.* **3**, 1616–1626 (2017). 10.1021/acsbiomaterials.7b00336
245. Habijan, T. *et al.* The biocompatibility of dense and porous Nickel–Titanium produced by selective laser melting. *Mater. Sci. Eng. C* **33**, 419–426 (2013). 10.1016/J.MSEC.2012.09.008
246. Günther, J. *et al.* On the effect of internal channels and surface roughness on the high-cycle fatigue performance of Ti-6Al-4V processed by SLM. *Mater. Des.* **143**, 1–11 (2018). 10.1016/J.MATDES.2018.01.042
247. Mohammadian, N., Turenne, S. & Brailovski, V. Surface finish control of additively-manufactured Inconel 625 components using combined chemical-abrasive flow polishing. *J. Mater. Process. Technol.* **252**, 728–738 (2018). 10.1016/J.JMATPROTEC.2017.10.020
248. Tan, K. L. & Yeo, S. H. Surface modification of additive manufactured components by ultrasonic cavitation abrasive finishing. *Wear* **378–379**, 90–95 (2017). 10.1016/J.WEAR.2017.02.030
249. Łyczkowska, E., Szymczyk, P., Dybała, B. & Chlebus, E. Chemical polishing of scaffolds made of Ti-6Al-7Nb alloy by additive manufacturing. *Arch. Civ. Mech. Eng.* **14**, 586–594 (2014). 10.1016/j.acme.2014.03.001
250. Zhang, J. *et al.* Cell responses to titanium treated by a sandblast-free method for implant applications. *Mater. Sci. Eng. C* **78**, 1187–1194 (2017). 10.1016/j.msec.2017.04.119
251. Amin Yavari, S. *et al.* Effects of bio-functionalizing surface treatments on the mechanical behavior of open porous titanium biomaterials. *J. Mech. Behav. Biomed. Mater.* **36**, 109–119 (2014). 10.1016/J.JMBBM.2014.04.010
252. Van Hooreweder, B., Apers, Y., Lietaert, K. & Kruth, J.-P. Improving the fatigue performance of porous metallic biomaterials produced by Selective Laser Melting. *Acta Biomater.* **47**, 193–202 (2017). 10.1016/J.ACTBIO.2016.10.005
253. Urlea, V. & Brailovski, V. Electropolishing and electropolishing-related allowances for powder bed selectively laser-melted Ti-6Al-4V alloy components. *J. Mater. Process. Technol.* **242**, 1–11 (2017). 10.1016/J.JMATPROTEC.2016.11.014
254. Amin Yavari, S. *et al.* Crystal structure and nanotopographical features on the surface of heat-treated and anodized porous titanium biomaterials produced using selective laser melting. *Appl. Surf. Sci.* **290**, 287–294 (2014). 10.1016/J.APSUSC.2013.11.069
255. Larsson, C. *et al.* Bone response to surface-modified titanium implants: studies on the early tissue response to machined and electropolished implants with different oxide thicknesses. *Biomaterials* **17**, 605–616 (1996). 10.1016/0142-9612(96)88711-4
256. Yao, C., Slamovich, E. B. & Webster, T. J. Enhanced osteoblast functions on anodized titanium with nanotube-like structures. *J. Biomed. Mater. Res. Part A* **85A**, 157–166 (2008). 10.1002/jbm.a.31551
257. Tobin, E. J. Recent coating developments for combination devices in orthopedic and dental applications: A literature review. *Adv. Drug Deliv. Rev.* **112**, 88–100 (2017). 10.1016/j.addr.2017.01.007
258. Goodman, S. B., Yao, Z., Keeney, M. & Yang, F. The future of biologic coatings for orthopaedic implants. *Biomaterials* **34**, 3174–83 (2013). 10.1016/j.biomaterials.2013.01.074
259. Bosco, R., Van Den Beucken, J., Leeuwenburgh, S. & Jansen, J. Surface Engineering for Bone Implants: A Trend from Passive to Active Surfaces. *Coatings* **2**, 95–119 (2012). 10.3390/coatings2030095

260. Zhang, B. *et al.* Bioactive Coatings for Orthopaedic Implants—Recent Trends in Development of Implant Coatings. *Int. J. Mol. Sci.* **15**, 11878–11921 (2014). 10.3390/ijms150711878
261. Civantos, A. *et al.* Titanium Coatings and Surface Modifications: Toward Clinically Useful Bioactive Implants. *ACS Biomater. Sci. Eng.* **3**, 1245–1261 (2017). 10.1021/acsbomaterials.6b00604
262. Amin Yavari, S. *et al.* Antibacterial Behavior of Additively Manufactured Porous Titanium with Nanotubular Surfaces Releasing Silver Ions. *ACS Appl. Mater. Interfaces* **8**, 17080–17089 (2016). 10.1021/acsam.6b03152
263. Yang, C., Huan, Z., Wang, X., Wu, C. & Chang, J. 3D Printed Fe Scaffolds with HA Nanocoating for Bone Regeneration. *ACS Biomater. Sci. Eng.* acsbomaterials.7b00885 (2018). doi:10.1021/acsbomaterials.7b00885 10.1021/acsbomaterials.7b00885
264. Ozhukil Kollath, V. *et al.* Electrophoretic deposition of hydroxyapatite and hydroxyapatite–alginate on rapid prototyped 3D Ti6Al4V scaffolds. *J. Mater. Sci.* **51**, 2338–2346 (2016). 10.1007/s10853-015-9543-6
265. Yu, P. *et al.* Bio-inspired citrate functionalized apatite coating on rapid prototyped titanium scaffold. *Appl. Surf. Sci.* **313**, 947–953 (2014). 10.1016/J.APSUSC.2014.06.113
266. Brie, I.-C. *et al.* Comparative in vitro study regarding the biocompatibility of titanium-base composites infiltrated with hydroxyapatite or silicatitanate. *J. Biol. Eng.* **8**, 14 (2014). 10.1186/1754-1611-8-14
267. Sing, S. L. *et al.* Fabrication of titanium based biphasic scaffold using selective laser melting and collagen immersion. *Int. J. Bioprinting* **3**, (2017). 10.18063/ijb.2017.01.007
268. Mróz, W. *et al.* In vivo implantation of porous titanium alloy implants coated with magnesium-doped octacalcium phosphate and hydroxyapatite thin films using pulsed laser deposition. *J. Biomed. Mater. Res. Part B Appl. Biomater.* **103**, 151–158 (2015). 10.1002/jbm.b.33170
269. Li, P., Warner, D. H., Fatemi, A. & Phan, N. Critical assessment of the fatigue performance of additively manufactured Ti–6Al–4V and perspective for future research. *Int. J. Fatigue* **85**, 130–143 (2016). 10.1016/J.IJFATIGUE.2015.12.003
270. Siddique, S. *et al.* Computed tomography for characterization of fatigue performance of selective laser melted parts. *Mater. Des.* **83**, 661–669 (2015). 10.1016/J.MATDES.2015.06.063
271. Webster, G. A. & Ezeilo, A. N. Residual stress distributions and their influence on fatigue lifetimes. *Int. J. Fatigue* **23**, 375–383 (2001). 10.1016/S0142-1123(01)00133-5
272. Wycisk, E., Emmelmann, C., Siddique, S. & Walther, F. High Cycle Fatigue (HCF) Performance of Ti-6Al-4V Alloy Processed by Selective Laser Melting. *Adv. Mater. Res.* **816–817**, 134–139 (2013). 10.4028/www.scientific.net/AMR.816-817.134
273. Qiu, C., Adkins, N. J. E. & Attallah, M. M. Microstructure and tensile properties of selectively laser-melted and of HIPed laser-melted Ti–6Al–4V. *Mater. Sci. Eng. A* **578**, 230–239 (2013). 10.1016/J.MSEA.2013.04.099
274. Wu, M.-W. & Lai, P.-H. The positive effect of hot isostatic pressing on improving the anisotropies of bending and impact properties in selective laser melted Ti-6Al-4V alloy. *Mater. Sci. Eng. A* **658**, 429–438 (2016). 10.1016/J.MSEA.2016.02.023
275. Greitemeier, D., Palm, F., Syassen, F. & Melz, T. Fatigue performance of additive manufactured TiAl6V4 using electron and laser beam melting. *Int. J. Fatigue* **94**, 211–217 (2017). 10.1016/J.IJFATIGUE.2016.05.001
276. Kahlin, M., Ansell, H. & Moverare, J. J. Fatigue behaviour of additive manufactured Ti6Al4V, with as-built surfaces, exposed to variable amplitude loading. *Int. J. Fatigue* **103**, 353–362 (2017). 10.1016/J.IJFATIGUE.2017.06.023
277. Styles, C. M., Evans, S. L. & Gregson, P. J. Development of fatigue lifetime predictive test methods for hip implants: Part I. Test methodology. *Biomaterials* **19**, 1057–1065 (1998). 10.1016/S0142-9612(98)00031-3

278. Tammas-Williams, S., Withers, P. J., Todd, I. & Prangnell, P. B. Porosity regrowth during heat treatment of hot isostatically pressed additively manufactured titanium components. *Scr. Mater.* **122**, 72–76 (2016). 10.1016/J.SCRIPTAMAT.2016.05.002
279. Kruth, J.-P., Deckers, J., Yasa, E. & Wauthlé, R. Assessing and comparing influencing factors of residual stresses in selective laser melting using a novel analysis method. *Proc. Inst. Mech. Eng. Part B J. Eng. Manuf.* **226**, 980–991 (2012). 10.1177/0954405412437085
280. Ali, H., Ma, L., Ghadbeigi, H. & Mumtaz, K. In-situ residual stress reduction, martensitic decomposition and mechanical properties enhancement through high temperature powder bed pre-heating of Selective Laser Melted Ti6Al4V. *Mater. Sci. Eng. A* **695**, 211–220 (2017). 10.1016/J.MSEA.2017.04.033
281. Shiomi, M., Osakada, K., Nakamura, K., Yamashita, T. & Abe, F. Residual Stress within Metallic Model Made by Selective Laser Melting Process. *CIRP Ann.* **53**, 195–198 (2004). 10.1016/S0007-8506(07)60677-5
282. Uddin, S. Z. *et al.* Processing and characterization of crack-free aluminum 6061 using high-temperature heating in laser powder bed fusion additive manufacturing. *Addit. Manuf.* **22**, 405–415 (2018). 10.1016/J.ADDMA.2018.05.047
283. Amin Yavari, S. *et al.* Fatigue behavior of porous biomaterials manufactured using selective laser melting. *Mater. Sci. Eng. C* **33**, 4849–4858 (2013). 10.1016/j.msec.2013.08.006
284. Hedayati, R., Hosseini-Toudeshky, H., Sadighi, M., Mohammadi-Aghdam, M. & Zadpoor, A. A. Multiscale modeling of fatigue crack propagation in additively manufactured porous biomaterials. *Int. J. Fatigue* **113**, 416–427 (2018). 10.1016/J.IJFATIGUE.2018.05.006
285. Hooreweder, B. Van, Lietaert, K., Neirinck, B., Lippiatt, N. & Wevers, M. CoCr F75 scaffolds produced by additive manufacturing: Influence of chemical etching on powder removal and mechanical performance. *J. Mech. Behav. Biomed. Mater.* **70**, 60–67 (2017). 10.1016/J.JMBBM.2017.03.017
286. LPW Technology. LPW Technology achieves ISO 13485 certification for the supply of additive manufacturing powders for medical applications - LPW Technology. (2015). Available at: <https://www.lpwtechnology.com/news/lpw-technology-achieves-iso-13485-certification-supply-additive-manufacturing-powders-medical-applications/>. (Accessed: 4th October 2018)
287. Arcam AB. AP&C receives ISO13485 certification - Arcam AB. (2017). Available at: <http://www.arcam.com/apc-receives-iso13485-certification/>. (Accessed: 4th October 2018)
288. F3049, A. I. Standard Guide for Characterizing Properties of Metal Powders Used for Additive Manufacturing Processes. *F3049 - 14* 1–3 (2014). doi:10.1520/F3049-14 10.1520/F3049-14
289. Slotwinski, J. A. *et al.* Characterization of Metal Powders Used for Additive Manufacturing. *J. Res. Natl. Inst. Stand. Technol.* **119**, 460 (2014). 10.6028/jres.119.018
290. Tang, H. P. *et al.* Effect of Powder Reuse Times on Additive Manufacturing of Ti-6Al-4V by Selective Electron Beam Melting. *JOM* **67**, 555–563 (2015). 10.1007/s11837-015-1300-4